International Water Management Institute

184

Research Report

Land Cover Changes in the Upper Great Ruaha (Tanzania) and the Upper Awash (Ethiopia) River Basins and their Potential Implications for Groundwater Resources

Kiran M. Chandrasekharan, Karen G. Villholth, Japhet J. Kashaigili, Gebrehaweria Gebregziabher and Paulo J. Mandela

Research Reports

The publications in this series cover a wide range of subjects—from computer modeling to experience with water user associations—and vary in content from directly applicable research to more basic studies, on which applied work ultimately depends. Some research reports are narrowly focused, analytical and detailed empirical studies; others are wide-ranging and synthetic overviews of generic problems.

Although most of the reports are published by IWMI staff and their collaborators, we welcome contributions from others. Each report is reviewed internally by IWMI staff, and by external reviewers. The reports are published and distributed both in hard copy and electronically (www.iwmi.org) and where possible all data and analyses will be available as separate downloadable files. Reports may be copied freely and cited with due acknowledgment.

About IWMI

The International Water Management Institute (IWMI) is an international, research-for-development organization that works with governments, civil society and the private sector to solve water problems in developing countries and scale up solutions. Through partnership, IWMI combines research on the sustainable use of water and land resources, knowledge services and products with capacity strengthening, dialogue and policy analysis to support implementation of water management solutions for agriculture, ecosystems, climate change and inclusive economic growth. Headquartered in Colombo, Sri Lanka, IWMI is a CGIAR Research Center with offices in 14 countries and a global network of scientists operating in more than 30 countries. www.iwmi.org

IWMI Research Report 184

Land Cover Changes in the Upper Great Ruaha (Tanzania) and the Upper Awash (Ethiopia) River Basins and their Potential Implications for Groundwater Resources

Kiran M. Chandrasekharan, Karen G. Villholth, Japhet J. Kashaigili, Gebrehaweria Gebregziabher and Paulo J. Mandela

International Water Management Institute (IWMI)
P. O. Box 2075, Colombo, Sri Lanka

The authors: Kiran M. Chandrasekharan is Senior Consultant at Indian Institute for Human Settlements, Bangalore, India. He was a GIS/RS Specialist at the International Water Management Institute (IWMI), Colombo, Sri Lanka, at the time this study was conducted; Karen G. Villholth is Director of Water Cycle Innovation (Pty) Ltd, Pretoria, South Africa. She was a Principal Researcher at IWMI, Pretoria, South Africa, at the time this study was conducted; Japhet J. Kashaigili is a Professor at Sokoine University of Agriculture, Morogoro, Tanzania; Gebrehaweria Gebregziabher is Assistant Professor of Development and Resource Economics, Department of Economics, Mekelle University, Mekelle, Ethiopia. He was a Research Economist at IWMI, Addis Ababa, Ethiopia, at the time this study was conducted; and Paulo J. Mandela was a Research Assistant at Sokoine University of Agriculture, Morogoro, Tanzania, at the time this study was conducted.

Chandrasekharan, K. M.; Villholth, K. G.; Kashaigili, J. J.; Gebregziabher, G.; Mandela, P. J. 2023. *Land cover changes in the Upper Great Ruaha (Tanzania) and the Upper Awash (Ethiopia) river basins and their potential implications for groundwater resources*. Colombo, Sri Lanka: International Water Management Institute (IWMI). 49p. (IWMI Research Report 184). doi: https://doi.org/10.5337/2023.212

/ land cover change / river basins / groundwater / water resources / land cover mapping / land use change / human settlements / rainfed farming / irrigated farming / irrigated areas variety / grasslands / woodlands / forest plantations / wetlands / catchment areas / vegetation index / moisture index / remote sensing / landsat / satellite imagery / datasets / algorithms / trends / climate change / urbanization / Africa South of Sahara / United Republic of Tanzania / Ethiopia /

ISSN 1026-0862
ISBN 978-92-9090-952-1

Please send inquiries and comments to IWMI-Publications@cgiar.org

A free copy of this publication can be downloaded at www.iwmi.org/publications/iwmi-research-reports/

Acknowledgements

The authors would like to thank Richard G. Taylor (Professor, Department of Geography, University College London, UK) for his critical inputs to this study and review of a previous version of this report. Behailu Birhanu (Addis Ababa University, Ethiopia) is thanked for providing geographic information system (GIS) data of the Upper Awash River Basin. Ashra Wickramathilaka (student intern from Moratuwa University, Sri Lanka) is acknowledged for the support provided with image processing. As partner of the GroFutures project, the Sokoine University of Agriculture (SUA) was responsible for the coordination of field observatories at the Makutapora wellfield in Dodoma, Tanzania, and in the Upper Great Ruaha River Basin, Tanzania, and for collecting data from responsible ministries and authorities. Also, SUA maintained constant engagement with the stakeholders and students working in the project.

Project

This study was undertaken as part of the *Groundwater Futures in Sub-Saharan Africa (GroFutures)* project, which is part of the Unlocking the Potential of Groundwater for the Poor (UPGro) program.

Collaborators

International Water Management Institute (IWMI)

Sokoine University of Agriculture, Morogoro, Tanzania

Donors

The UPGro program (IWMI Grant No. NE/M008266/1) was funded by the Natural Environment Research Council (NERC), UK, and the Economic and Social Research Council (ESRC), UK.

This research was carried out as part of the CGIAR Research Program on Water, Land and Ecosystems (WLE) and supported by Funders contributing to the CGIAR Trust Fund (https://www.cgiar.org/funders/).

Contents

Acronyms and Abbreviations

BUI	Built-up Index
CHIRPS	Climate Hazards group InfraRed Precipitation with Stations
DEM	Digital Elevation Model
ETM	Enhanced Thematic Mapper
GPS	Global Positioning System
IRA	Institute of Resource Assessment
LaSRC	Land Surface Reflectance Code
LEDAPS	Landsat Ecosystem Disturbance Adaptive Processing System
MODIS	Moderate Resolution Imaging Spectroradiometer
MSAVI	Modified Soil Adjusted Vegetation Index
NDBI	Normalized Difference Built-up Index
NDMI	Normalized Difference Moisture Index
NDVI	Normalized Difference Vegetation Index
NIR	Near Infrared
OLI	Operational Land Imager
RNP	Ruaha National Park
SAVI	Soil Adjusted Vegetation Index
SRTM	Shuttle Radar Topography Mission
SWIR	Shortwave Infrared
TIRS	Thermal Infrared Sensor
TM	Thematic Mapper
UARB	Upper Awash River Basin
UGRRB	Upper Great Ruaha River Basin
USGS	United States Geological Survey

Summary

Unprecedented resource demands due to population growth, increasing food demand and urbanization, exacerbated by climate change, have led to unsustainable development pathways in many parts of the world. Information about the status and trends of land and water resources is a critical requirement for long-term policies and strategies for equitable and sustainable development. Satellite remote sensing offers cost-effective, rapid and reproducible methods to monitor indirectly the utilization patterns and trends of several natural resources such as land and water resources.

This report presents the results of a land cover change analysis conducted in two headwater catchments of river basins in sub-Saharan Africa, where impoverished communities critically depend on local land and water resources: the Upper Great Ruaha River Basin (UGRRB) in Tanzania (20,823 km^2, approx. 800,000 people) and the Upper Awash River Basin (UARB) in Ethiopia (10,695 km^2, approx. 5.3 million people). The two basins represent areas which are significantly different in terms of agricultural development and patterns of water resource use. UARB represents an agricultural region, which has emerging commercial farms, expanding urban centers and threatened natural vegetation. UGRRB still has significant areas under natural vegetation but expanding areas under irrigation. In UGRRB, surface water is the main source of irrigation water, while in UARB, groundwater resources are increasingly used for irrigation by smallholder farmers and commercial farms.

Land cover changes were assessed over a 15 to 20 year period up to 2015 or 2016 using land cover maps at the start and end of the period. Changes in UGRRB were analyzed between 1994-1995 and 2015-2016 (20-year period) and changes in UARB were assessed between 2000 and 2015 (15-year period). Land cover maps were prepared using remote sensing imagery, secondary maps and ground truth information. Satellite imagery from various Landsat sensors with a spatial resolution of 30 m was used. A post-classification change analysis was conducted to estimate the changes in each land cover type and the patterns of land cover transitions between different categories.

In general, both basins witnessed an expansion of agricultural areas at the expense of natural land cover, as well as an expansion of human settlement/urban areas at the expense of natural land cover and rainfed agricultural areas. The UGRRB still possesses significant areas under natural land cover (75% in 2015-2016), but such natural land cover has almost vanished in the UARB (15% in 2015). A transition from natural land cover to rainfed agriculture is the prominent trend in UGRRB. An increase in irrigated agriculture and expansion of human settlement/urban areas from previously rainfed agricultural lands are the dominant trends observed in the UARB.

This study provides detailed results of the nature of land cover transitions in the two basins. The results show that the land cover changes are not a unidirectional phenomenon except in heavily built environments (human settlements) and irrigated agriculture, but follow multiple trajectories, providing important insights about the changing land use patterns. The analysis further shows that patterns of land use change in the UGRRB and UARB resemble those of the general patterns witnessed in many low-income countries. The patterns represent different, successive stages of development from agropastoral systems to urbanized areas and more intensive farming systems, with the UARB being more developed, while the UGRRB being more vulnerable to further development.

This vulnerability is also reflected in the realized and remaining potential for groundwater development in the two basins. The UGRRB, though less developed in terms of groundwater withdrawals for irrigation, will likely be more sensitive to the environmentally harmful impacts of intensifying groundwater-irrigated agriculture, due to the local and downstream presence of critical and protected terrestrial and wetland ecosystems.

Land Cover Changes in the Upper Great Ruaha (Tanzania) and the Upper Awash (Ethiopia) River Basins and their Potential Implications for Groundwater Resources

Kiran M. Chandrasekharan, Karen G. Villholth, Japhet J. Kashaigili, Gebrehaweria Gebregziabher and Paulo J. Mandela

Introduction

Improved access to water, food and health services has helped to increase life expectancy in many parts of the world. The world population has grown by 1 billion people in the last 10-15 years, and the current global population of 7.3 billion is expected to reach 9.7 billion by 2050 (UN DESA 2015). Finite natural resources of the world are under pressure due to the increasing requirements of the growing population for food, freshwater and energy. Over the past 50 years, humans have changed ecosystems more rapidly and extensively than in any comparable period of time in human history (Millennium Ecosystem Assessment 2005; IPBES 2019). The technological developments and increased economic and trade activities have enabled and accelerated the use of natural resources. These sustained and intensive human interactions with land and water resources have resulted in substantial gains in human well-being. However, achievements in economic growth in some regions have been associated with degradation of land and water resources as well as deterioration of related ecosystem goods and services, such as biomass, carbon storage, soil health, water storage and supply, biodiversity, and social and cultural services (FAO 2011).

Intensive resource utilization is reflected in rapid changes in land use and land cover. Globally, agriculture, plantations, pastures and urban areas have expanded in recent decades at the cost of natural landscapes. Agriculture currently uses about ca. 11% of the world's land surface, and the net cultivated area (land under agricultural crops) has grown by 12% over the last 50 years, mostly at the expense of forest, wetland and grassland habitats (FAO 2011). Only biomes relatively unsuitable for agriculture, such as deserts, boreal forests and tundra, have remained largely untransformed by human action (Millennium Ecosystem Assessment 2005). While agriculture and pastures are the most extensive forms of land use change (Lambin and Meyfroidt 2011), urbanization of land surfaces is one of the most irreversible human impacts on the global biosphere (Seto et al. 2011). Urbanization not only results in the loss of natural and agricultural lands, but also significantly changes hydrological systems and affects local biodiversity; it also presents opportunities for efficient resource use and management.

Africa has the highest rate of population growth among major geographical regions, increasing at a pace of 2.6% annually during the period 2010-2015 (UN DESA 2015). Matima et al. (2009) reported that the major form of land use change in East Africa is the conversion of natural land cover to agricultural areas and identified the major driver for this change as the need to address food security, particularly through large-scale farming. Urbanization in Africa is largely attributed to population growth rather than the gross domestic product (GDP) growth rate (Seto et al. 2011).

Changes in land use and land cover could detrimentally affect water resources in the region, not only by altering replenishment, storage and demand patterns but also by affecting risks to water-related disasters such as floods and droughts. It has been found that the influence of large-scale land use change on groundwater recharge may be more pronounced over the next decades than climate change (Favreau et al. 2009; Taylor et al. 2013). With the increasing reliance on groundwater for domestic use and economic (agricultural and industrial) development in Africa (Braune and Xu 2010), there is a need to understand how land use change affects groundwater use and resource availability, primarily through recharge processes, amounts and quality of water, and how land use policies could be informed by the availability and renewability of water resources, especially groundwater.

Objectives

Sub-Saharan Africa is one of the poorest regions in the world. Sustainable use of land and water resources is critical for poverty alleviation in the region, especially under scenarios of a changing climate and increasing water demand. Developing sustainable resource utilization strategies requires updated information and continuous monitoring of the status of the resources and trends in water use.

The objective of this study is to quantify historical trends and patterns of land use and land cover change at the distributed river basin scale in sub-Saharan Africa. Such analyses inform quantitative evaluations of the sustainability of resource use pathways and susceptibility to degradation under conditions of various drivers. The study was conducted in two river basins: (i) the Upper Great Ruaha River Basin (UGRRB) in Tanzania, and (ii) the Upper Awash River Basin (UARB) in Ethiopia. A key focus of these analyses is the identification of trends or patterns in agricultural areas and human settlements, which are susceptible to intensive utilization of land and water resources.

The scope of the analysis is mostly limited to identifying the patterns of land cover transition and estimating the changes that occurred in the recent past. While identifying the specific drivers of various patterns of land use change is beyond the scope of this analysis, some of the major socioeconomic processes driving the overall transitions at basin level are explored. Finally, the report describes how the observed land use and land cover changes may impact groundwater resources in the study basins.

Study Areas

Upper Great Ruaha River Basin

The Upper Great Ruaha River Basin (UGRRB) is part of the Rufiji River Basin of Tanzania, which covers an area of about 83,970 km² (NEMC 2006) (Figure 1). The UGRRB lies between longitudes 33° 30.9' E to 35° 35.7' E and latitudes 7° 18.7' S to 9° 35.5' S and covers an area of 20,823 km². The lower discharge point of UGRRB is at the outflow from the wetland at NG'iriama (Kashaigili et al. 2006a). The altitude of the UGRRB ranges from 1,003 meters above mean sea level (mamsl) to 2,966 mamsl, with the higher altitude regions located in the southern part of the basin. The mean annual rainfall ranges from 500 mm to 1,600 mm, which is received in a single rainfall season extending usually during the period between late November and June (Kashaigili et al. 2006a). The mean annual potential evapotranspiration is around 1,900 mm (SMUWC 2001a). The long-term mean annual runoff at about 80 km downstream of the basin outlet (Msembe Ferry) is 2,442 million cubic meters (Mm³) (Kashaigili et al. 2006a).

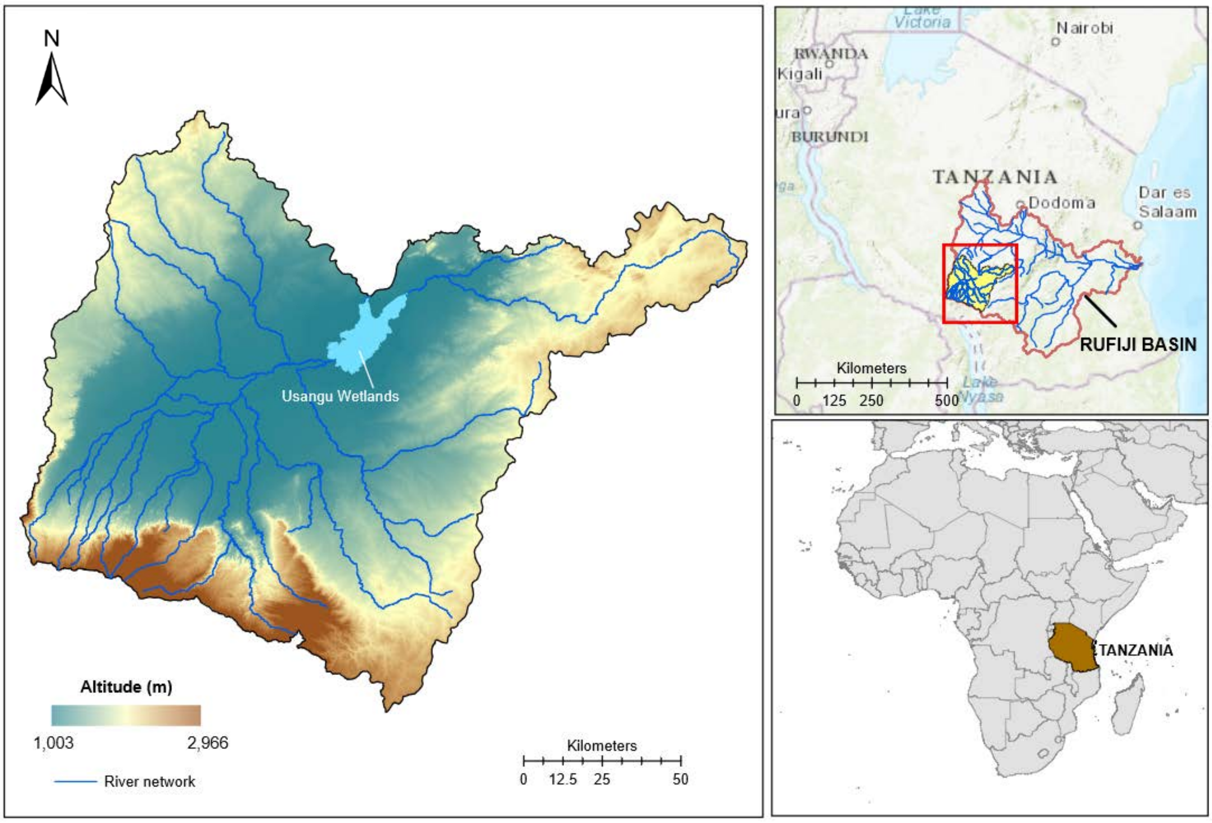

Figure 1. Upper Great Ruaha River Basin in Tanzania – location and altitude ranges.

Sources: The altitude map is based on Shuttle Radar Topography Mission (SRTM) Digital Elevation Model (DEM) (NASA JPL 2013); the background map in the inset is from ArcGIS base maps; and the country boundaries are from FAO (2015).

The Upper Great Ruaha River is a major tributary to the Rufiji River. The headwaters rise in the Kipengere mountains in southwest Tanzania and drain through the broad alluvial Usangu plains and the Ruaha National Park. The Rufiji River runs for about 600 km and drains to the Indian Ocean in an easterly direction. The Usangu plains encompass the Usangu wetland (about 1,800 km^2 area), which is one of the most valuable ecosystems in Tanzania from a conservation perspective. The wetland provides habitat to a large number of flora and fauna, and supports numerous livelihood activities such as agriculture, pastoralism, fisheries and small-scale industries (Kashaigili et al. 2006b).

The major land cover types in the UGRRB include natural forests and woodlands, savanna grasslands, bushlands, wetlands and agriculture. Major crops in the region are rice, vegetables and maize, of which rice is irrigated, and the others are cultivated under rainfed conditions. There was a rapid expansion in the irrigated area (about 10,000 ha to 40,000 ha) near the Usangu wetlands between 1970 and 2000 (SMUWC 2001a; Kashaigili et al. 2006b). While the total population of the Rufiji River Basin is approx. 6 million (Mwakalila 2011), the study area (UGRRB) is home to approx. 800,000 people (CIESIN 2017) with a population density of 38/km^2. Over the last few decades, the increasing demand for agricultural land due to population growth has led to the clearance of natural vegetation and degradation of soil, wetlands and water resources (Taylor et al. 2011).

Upper Awash River Basin

The Awash River Basin is a major drainage system in Ethiopia, extending to about 110,000 km^2 (Figure 2). The river originates in the Ginchi area in the West Shewa region of central-west Ethiopia and flows for a length of about 1,200 km. Unlike most rivers in Ethiopia, which flow towards south or west, Awash is the only major river flowing towards the northeast. Most other rivers have higher annual flows compared to Awash, but flow mostly through canyons and deep valleys and are thus largely inaccessible for direct human use; sections of the Awash River are relatively accessible and offer greater possibilities for human utilization (FAO 1965).

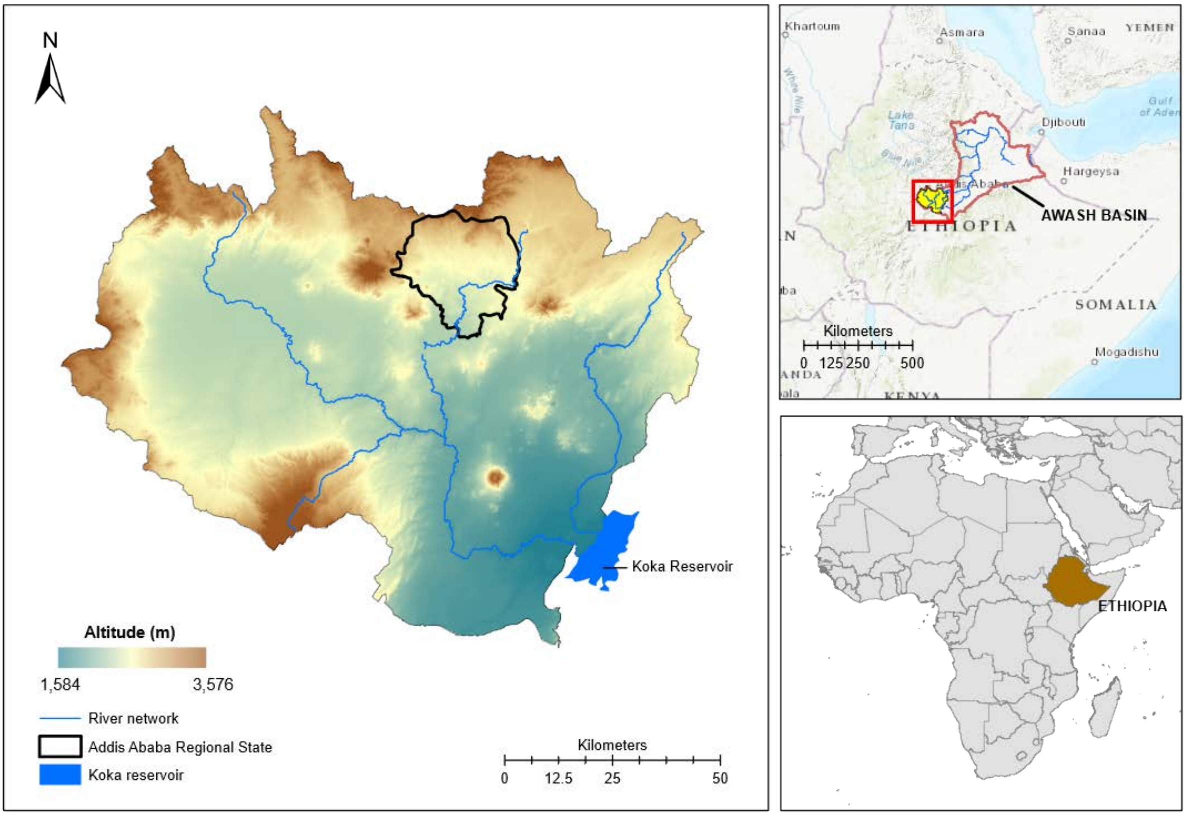

Figure 2. Upper Awash River Basin in Ethiopia – location and altitude ranges.

Sources: The altitude map is based on Shuttle Radar Topography Mission (SRTM) Digital Elevation Model (DEM) (NASA JPL 2013); the background map in the inset is from ArcGIS base maps; and the country boundaries are from FAO (2015).

The annual rainfall of the Awash River Basin varies from about 1,600 mm near its origin to 160 mm close to the northern limit of the basin with a mean of 850 mm. Rainfall is bimodal, with the main rainfall season occurring from June to September and a shorter, less intensive rainfall season occurring from March to April. The mean annual potential evapotranspiration ranges from 1,810 mm in the upper basin to 2,348 mm in the lower part (Berhe et al. 2013). The long-term mean annual runoff of the Awash Basin is about 4,900 Mm^3 (Edossa et al. 2010).

This study was conducted in the upper headwater catchment of the Awash River Basin, which drains to the Koka reservoir. The UARB is located between longitudes 37° 57.0 E to 39° 17.5' E and latitudes 8° 11.2' N to 9° 19.0' N and covers an area of 10,695 km^2. The altitude ranges from 1,584 mamsl to 3,576 mamsl.

Geographically, agriculture is the largest land cover type in the UARB. Bushland and grassland also cover significant areas of the basin. However, with Addis Ababa city (the capital of Ethiopia) located within the basin, the most prominent land use in UARB is urban areas. The basin also has several other townships and industrial establishments.

The population of UARB in 2015 was approx. 5.3 million, of which approx. 3.1 million lives within the Addis Ababa Regional State (Figure 2). While the population density of UARB is 497/km^2, the area outside Addis Ababa Regional State has a population density of 213/km^2.

Methods and Data Sources

Land cover change in human-modified landscapes is a continuous process, influenced by a multitude of socioeconomic, political and climatic factors. Remote sensing technology has been widely used to develop land cover maps and assess the land cover changes over time. With an array of satellite sensors providing repeated coverage of the Earth's surface, advancements in processing algorithms and computational power, and with extended periods of data availability, remote sensing offers increasingly efficient tools to assess land cover changes. Although the UARB and UGRRB are quite different with respect to the patterns of land use, and changes as well as the factors influencing them, the challenge is to identify comparable techniques for assessing these changes over similar time frames. Both basins are agrarian in nature with a significant presence of smallholder farms and small townships, while the large conurbation of Addis Ababa is unique to UARB (Figure 2). Moderate resolution datasets such as Landsat images (30 m) are suitable to characterize the changes in basins of this magnitude and with these types of landscapes. Time periods were decided based on the requirements of the study and data availability. While higher resolution images such as Sentinel-2 MultiSpectral Instrument (MSI)[1] from the European Space Agency (ESA) are available in later time periods, Landsat images offer the best resolution in a cost-effective way for earlier time periods. It was decided to use Landsat images for the mapping of all the time periods to obtain a consistent resolution suitable for the change analysis. Land cover maps from secondary sources based on Landsat images of earlier time periods were also used for the analysis. The time periods selected enable a change analysis to be carried out for approximately the last 15 to 20 years, which represent a period of unprecedented changes.

Methodology

For each river basin, land cover changes were estimated using land cover maps of two time slices. Changes in the UGRRB were analyzed between the periods 1994-1995 and 2015-2016 (20 years), whereas changes in the UARB were analyzed between 2000 and 2015 (15 years). Land cover maps were prepared for each time period using remote sensing imagery acquired, secondary maps and ground truth information.

Land cover classification of complex, human-modified landscapes using satellite imagery often requires multiple approaches and datasets. The accuracy of the classification relies upon the spectral reflectance properties and the distinguishability of distinct land cover types at the sampled locations. The classification is performed by analyzing the similarity between the spectral reflectance pattern of an area or pixel and the signatures of various land cover types derived from sample locations. In other words, the success of the classification depends upon the statistical separability of signatures of various land cover types. It is essential to develop signatures that represent the land cover types accurately and uniquely. In landscapes where mixed land cover is present and interspersed at a finer scale, the signature development that satisfies this requirement is a challenging process, and obviously depends on the

[1] Sentinel-2 Multispectral Imagery from ESA. The images are available at 10 m, 20 m and 60 m resolution for various bands.

spatial scale of the analysis. Sample data for signature development may be gathered from image interpretation, ground measurements or any other trusted or verified source of information (Egorov et al. 2015).

Analysts often modify and adapt the standard datasets and algorithms to enhance the signature separability. A single image is a snapshot of the land cover at a particular time that the image was captured. However, an important characteristic of vegetation cover is the intra-annual variation of biomass across different seasons. Therefore, the variability in seasonal changes between different land cover types can be used as an important complementary input to enhance the differentiation between spectral signatures of various land cover types. Several studies have included images from multiple seasons within a year, or over several years, in the classification process (Krishnaswamy et al. 2004; Senf et al. 2015).

Multispectral images from various Landsat sensors were used for this study. Various vegetation, soil moisture and urban/built-up indices derived from multi-seasonal Landsat data were used along with the multispectral bands of the images. Details of the Landsat images and the spectral indices used for this study are provided in the section *Data Sources*. The diagram in Figure 3 illustrates the datasets and methods used for developing the classified land use maps.

The images were classified using the supervised classification techniques Random Forest Classification (Breiman 2001) and Maximum Likelihood Classification (Settle and Briggs 1987). Parametric classification approaches such as Maximum Likelihood Classification are often less efficient in heterogeneous landscapes, where it is difficult to obtain a sufficient number of homogeneous sample locations required for developing spectral signatures with a normal distribution. Ensemble learning algorithms such as Random Forest Classification (Breiman 2001) have been producing better results for such landscapes. In this study, the Maximum Likelihood Classifier algorithm was used in UARB, and the Random Forest Classifier algorithm was used for the more heterogeneous landscape of UGRRB. Analysis in terms of classification and mapping for the two time periods in each basin was performed systematically and consistently, enabling easy comparison of temporal changes.

Ground truth information collected through contemporary field surveys and from secondary sources, high-resolution images from Google Earth, visual interpretation of the images used for classification, and secondary maps were all used as supportive material for the classification. The results were visually cross-checked with Google Earth and Landsat images and refined through iterative manual editing. Agricultural areas were classified through a two-step process. The entire agricultural area was considered as a single category in the first step using the supervised classification techniques. Subsequently, the agricultural areas were classified into irrigated and rainfed areas using spectral indices such as Normalized Difference Vegetation Index (NDVI) and Normalized Difference Moisture Index (NDMI) (see section *Spectral Indices for Classification*), capturing the seasonal vegetation and moisture status of agricultural areas.

A post-classification change analysis was carried out to estimate the transition of land use and land cover from the earlier time period to the later time period. The method involves separately classifying images from different time periods to develop land use maps and compare the classified images, pixel by pixel, to assess the temporal change. This analysis minimizes the atmospheric impacts on the multi-temporal images and provides information on the quantity and spatial distribution of change and transition from one land class to another (Lu et al. 2004).

Overall, this study follows the approaches used by several earlier studies that employed seasonal change information captured in multi-seasonal images for land cover classification (e.g., Mtibaa and Irie 2016), and well-established procedures for post-classification change analysis. However, appropriate modifications were incorporated in the procedures to suit the land cover characteristics of each of the basins, especially for the segregation of irrigated and rainfed areas.

Data Sources

Remotely sensed data from Landsat satellites were used for the preparation of land cover maps for different time periods. Landsat 8 Operational Land Imager (OLI) and Thermal Infrared Sensor (TIRS)[2] data were used for developing land cover maps for the period 2015-2016 for both basins. Landsat 7 Enhanced Thematic Mapper Plus (ETM+) data were used for the year 2000 for the UARB, and Landsat 5 Thematic Mapper (TM) images were used to modify an existing land cover map of 1994 to develop the land cover map for the period 1994-1995 for the UGRRB.

The standard Landsat Level-1 products and the atmospherically corrected surface reflectance data products (Level-2) (USGS 2015, 2016a) of these sensors were downloaded from the online satellite data archive EarthExplorer (USGS 2016b). The characteristics of Landsat images used are provided in the Appendix.

Spectral Indices for Classification

Landsat surface reflectance data products provided by the United States Geological Survey (USGS) were used to develop various spectral indices for the classification. Surface reflectance data are produced after the removal of atmospheric effects on satellite data, which enables comparison of data acquired from various locations and for different time periods. The surface reflectance data

[2] OLI, TIRS, ETM+ and TM refer to sensors aboard Landsat satellites.

for Landsat 5 and 7 are developed using the Landsat Ecosystem Disturbance Adaptive Processing System (LEDAPS) (USGS 2020a), whereas Landsat 8 OLI surface reflectance data are generated through the Landsat 8 Land Surface Reflectance Code (LaSRC) algorithm (USGS 2020b).

Normalized Difference Vegetation Index (NDVI)

Normalized Difference Vegetation Index (NDVI) is one of the most widely used spectral indices derived from remote sensing data for vegetation studies. NDVI is highly correlated with many vegetation parameters, such as crown closure, leaf vigor, and canopy biomass and leaf area index, and is the most robust of the vegetation

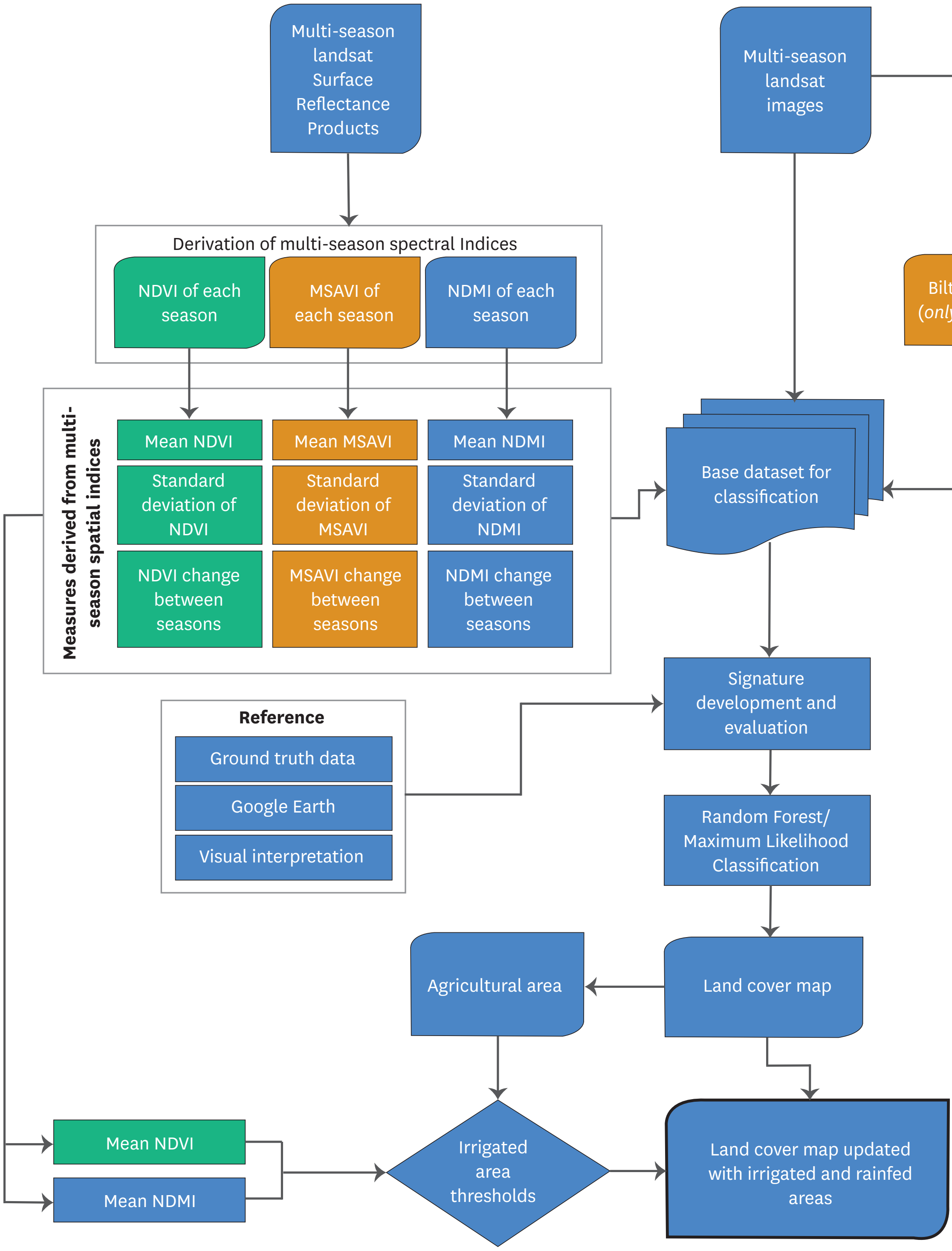

Figure 3. Method of land use classification using multi-seasonal satellite images.

Note: NDVI – Normalized Difference Vegetation Index; NDMI – Normalized Difference Moisture Index; MSAVI – Modified Soil Adjusted Vegetation Index.

indices developed (Lyon et al. 1998). Variability in NDVI across seasons estimated from multi-seasonal satellite imagery can be used to study the phenological variations in land cover (Reed et al. 1994).

Most land cover types in UGRRB and UARB exhibit a seasonal change. NDVI derived from multi-seasonal images provides estimates of the abundance and density of the vegetation and the seasonal change in various vegetation types.

NDVI is calculated as a ratio involving the reflections in the two spectrums: Red (RED) and Near Infrared (NIR), using Equation (1):

$$NDVI = \frac{(NIR - RED)}{(NIR + RED)} \quad (1)$$

Modified Soil Adjusted Vegetation Index (MSAVI)
Values of vegetation indices such as NDVI can be affected by the reflectance from exposed soil surface, where the vegetation cover is low. The Soil Adjusted Vegetation Index (SAVI) was developed to minimize the influence of soil on vegetation reflectance by incorporating a constant soil adjustment factor L into the NDVI equation (Huete 1988). The Modified Soil Adjusted Vegetation Index (MSAVI) is a modified version of SAVI, which replaces the soil adjustment factor L (which requires prior information about the vegetation densities of the area) with a self-adjusting L factor and hence does not require prior knowledge of the vegetation densities (Qi et al. 1994).

From grasslands and bushlands to agricultural areas and plantations, most areas of the study basins have a significant presence of exposed soil. MSAVI provides an important measure of vegetation spectra in these areas. The MSAVI values, in combination with NDVI values, provide estimates of the densities and variations of vegetation in various land cover types. MSAVI is calculated using RED and NIR values with an inductive L function applied to maximize the reduction of soil effects on the vegetation signal (Qi et al. 1994).

$$MSAVI = \frac{1}{2}\left(2 \times NIR + 1 - \sqrt{(2 \times NIR + 1)^2 - 8 \times (NIR - RED)}\right) \quad (2)$$

Normalized Difference Moisture Index (NDMI)
NDMI estimates moisture levels stored in vegetation. The index is derived based on the absorption of water by the Shortwave Infrared (SWIR) band compared to the NIR band (Wilson and Sader 2002). NDMI was included as a variable in the classification to capture the seasonal moisture variations in vegetation in various seasonally changing land cover types.

NDMI is calculated using NIR and SWIR bands using Equation (3):

$$NDMI = \frac{(NIR - SWIR)}{(NIR + SWIR)} \quad (3)$$

For Landsat 5 and 7, band 5 was used as the SWIR band, and for Landsat 8, band 6 was used as the SWIR band (USGS n.d.[a]).

Land Cover Classification and Change Analysis

Classification Scheme

The land cover classification scheme adapted for the two catchments was broadly similar with some variations to suite respective local conditions. Land cover categories were decided based on discussions held with a group of researchers familiar with the areas and on the visual exploration of the images. The definitions were mainly adopted from Vesa et al. (2011), but modified to include additional categories to represent the actual land types present in the study basins.

The ten land cover classes identified for mapping are given below:

1. **Irrigated agriculture**: *Cultivated areas, which receive irrigation to support the water requirements, at least for one crop cycle in a year*
2. **Rainfed agriculture**: *Cultivated areas which receive water directly from rainfall without any human intervention*
3. **Grassland**: *Open areas dominated by grass. Trees and bushes may occur on less than 10% of the area*
4. **Bushland**: *Predominantly comprised of plants that are multi-stemmed from a single root base*
5. **Woodland**: *Tree-dominated ecosystems with canopy cover ranging from 20% to 80%, and characterized by only two main strata - the main canopy itself and a shrub/herb-layer beneath*
6. **Natural forest**: *A continuous stand of trees with a diversity of cover types. Natural forest has three canopy layers: emergent, middle and lower canopy*
7. **Forest plantation**: *Monoculture tree plantations*
8. **Human settlement**: *Residential or commercial areas and associated built-up structures, which may be interspersed with small farmlands and tree clusters*
9. **Wetland**: *Waterlogged and seasonally inundated areas, which may bear grasses and herbaceous vegetation seasonally*
10. **Water body**: *Inland water bodies including lakes and rivers*

Mapping of UGRRB includes all ten categories, while forest plantation and woodland were not included in the mapping of UARB. The 'forest' class in UARB does not always exhibit all the characteristics of the natural forest class as defined here due to the fragmented nature and may therefore include tree clusters rather than a continuous stand of trees.

Data

Satellite Images

Landsat images acquired for multiple dates representing different seasons were used for classification of the scenes. The advantage of using multi-seasonal imagery over single date imagery for classification purposes is that the former is more likely to capture the seasonal variations of vegetation and is likely to enhance the spectral variability required for the classification.

Three Landsat scenes are required to cover UGRRB (Figure 4), whereas two scenes are needed for mapping UARB (Figure 5). The extent of the scenes and scene overlap are shown in Figures 4 and 5. For UGRRB, the overlap area was mapped using the 169/66 scene, which covers majority of the area. The scene 168/54 was used for the overlap areas between the scenes in UARB.

Since agriculture is an important category of the analysis, images acquired during the crop season are the most appropriate for the classification (Wardlow and Egbert 2008). However, since much of the crop season of the region corresponds with the rainfall season, the availability of cloud-free images for the study period was limited. Images for three dates per basin, period, sensor and scene were selected for the analysis taking into consideration the availability of cloud-free images and temporal correspondence with crop seasons (Table 1). The dates were selected to approximately represent pre-sowing, full crops/growing, and post-harvest conditions of the crops. These three dates are also suitable to capture the seasonal changes in natural vegetation in the basin. However, for some of the scenes for the earlier period, images for only one or two seasons were available due to cloud cover. The small northern area in UGRRB (Figure 4) covered by the scene 169/65 is mostly woodlands and did not require complex classification routines to prepare the land cover map. The image from only one season was used for this scene.

Ground truth Data

Ground truth datasets for classification of the selected satellite images were gathered from three sources: (i) field surveys providing Global Positioning System (GPS) coordinates and visual information on land cover, (ii) high resolution images in Google Earth, and (iii) secondary maps.

Field Surveys
Primary field surveys were conducted by the project team in UGRRB during June 2016 to collect GPS coordinates and associated land cover information from various land cover categories in a spatially representative manner. For UARB, GPS coordinates of irrigated croplands were collected from government agencies.

For UGRRB, the field survey followed the most optimal route to collect information from various parts of the basin and to cover all major land use and land cover types. Despite accessibility constraints spatially limiting the data collection to areas accessible by roads, samples from all major land cover categories were obtained. A total of 200 locations were sampled to collect the ground truth information. A 'location' consisted of a plot larger than 60 m x 60 m with approximately uniform land use. Part of the survey data was used for training the classifier and the remaining was used for validating the results (see sections *Land Cover Classification for the Late Time Period* and *Accuracy Assessment*).

While some of the plots had multiple land cover types, care was taken to ensure that the assigned land cover was dominant enough to consider the plot as a representative sample for that land cover category. The plot size corresponds to 2 x 2 pixels of Landsat imagery. GPS locations were recorded near the center of the sampled area. For agricultural areas, additional information such as crop types, crop seasons and water source(s) over the year was also recorded. Assessments of plot size, location of the plot center and percentage of land cover types were based on approximate visual estimations.

For UARB, data from 79 locations with irrigated agriculture were obtained from the Ministry of Agriculture, Ethiopia. The survey methods used for the collection of these plot data are not known. Ten of these locations were used for training the irrigated area classification. The remaining locations were used for validation of the classification of agricultural areas into irrigated and rainfed areas (see sections *Classification of Irrigated Areas* and *Accuracy Assessment*).

Google Earth Images
The high-resolution images (up to 0.65 m) available in Google Earth[3] were used for developing classification training sites in areas where primary ground truth data were not available. Google Earth data were also used for verification and refining of the classification outputs. Although the images are of a very high resolution, it is not possible to conclusively determine certain land cover categories solely based on Google Earth images. This is particularly true for determining the irrigation status of agricultural areas. Since GPS coordinates were available for some of the land cover classes in UGRRB, Google Earth was primarily used to identify croplands in general and

[3] Google Earth is a web-based program that provides visualization of the Earth using satellite imagery (https://www.google.com/earth).

Figure 4. Landsat scenes used for the classification of UGRRB.

Figure 5. Landsat scenes used for the classification of UARB.

for developing training sites for woodlands, bushlands and human settlements. In UARB, sample locations for classifying croplands, urban areas and various natural vegetation classes were obtained from Google Earth.

Secondary Maps

A land cover map of UGRRB in 1994 (Figure 6) prepared by the Institute of Resource Assessment (IRA), Tanzania, was used as a base map for preparing the map for the period 1994-1995. This base land cover map was prepared using a Landsat 5 TM image acquired on August 14, 1994, with nine land cover categories. These categories are mostly similar to the land cover classes defined for the current classification scheme (see section *Classification Scheme*). The permanent swamp and urban areas mapped in the earlier classification are similar to the wetland and human settlement areas in the new classification, respectively. The remaining classes are comparable in both classification schemes, except that the old map does not distinguish between irrigated and rainfed agricultural areas. The land cover categories in the 1994 map were represented by IRA using significant generalization. Spatial lumping of land cover areas in maps derived from remote sensing is a common practice to remove unwanted local variations and thus improve the spatial coherence and visual appearance (Fierens and Rosin 1994). As a result, many areas with a complex land cover mixture appear relatively uniform in the map. At the same time, the map provides an excellent broad overview of the land use and land cover of that period. The 1994-1995 map for this study was prepared by modifying the 1994 map by retaining the complexity of the land cover pattern at a much finer scale and including additional categories such as irrigated and rainfed agriculture using satellite images of the same period (Landsat 5 TM, Table 1).

Land Cover Classification for the Late Time Period

Data Preparation

One cloud-free image for each scene was selected as a primary image for the classification process. A set of additional variables derived from multi-season satellite images was also used along with this primary image to incorporate information on seasonal changes in the classification process.

Images from the following dates were used as the primary images for the classification for each scene (Table 1):

Upper Great Ruaha River Basin

- 168/66: May 16, 2016
- 169/65: June 23, 2016
- 169/66: May 6, 2016

Upper Awash River Basin

- 168/54: December 23, 2015
- 169/54: December 30, 2015

The Landsat 8 (OLI and TIRS) imagery has 11 spectral bands. Seven spectral bands, from 2 to 7 and band 10, were selected for the classification process. Band 1 (coastal/aerosol), band 8 (panchromatic) and band 9 (cirrus) were not used for the classification because these bands have limited information to classify land cover. Similarly, only one band (band 10) out of the two thermal bands (bands 10 and 11) was selected for the classification.

Derivation of Seasonal Variables

As described earlier (see section *Spectral Indices for Classification*), the Landsat 8 surface reflectance data products available from USGS EarthExplorer were used to derive various spectral indices. NDVI and NDMI were derived for each image of the three stages of the crop growing period selected for both basins. In addition, for UGRRB, MSAVI was derived for each of the multi-season images. A set of four measures per pixel was calculated over the cropping season based on these multi-date spectral indices to quantify the seasonal variations, i.e., seasonal mean, seasonal standard deviation, and two change layers between successive pairs of images (pre-sowing to full crops; full crops to post-harvest) to represent two change trajectories (Krishnaswamy et al. 2004). While the multi-season mean of these spectral indices represents the quantity of the measured phenomena, the standard deviation and the change layers are representations of seasonal changes of each measured variable. Finally, for UARB, a built-up index (BUI) was also calculated using the method proposed by He et al. (2010) for the primary image selected. The method initially calculates a Normalized Difference Built-up Index (NDBI) (Zha et al. 2003) and then calculates the BUI by subtracting the NDVI from NDBI.

$$NDBI = \frac{(SWIR - NIR)}{(SWIR + NIR)} \tag{4}$$

$$BUI = NDBI - NDVI \tag{5}$$

These additional variables were appended to the primary Landsat 8 OLI/TRS layer stack, which was used as the input imagery dataset for the classification.

Classification of Satellite Images

The land cover classification of UGRRB was performed using the Random Forest Classifier in the Google Earth Engine[4] platform, whereas the classification of UARB was done using the ERDAS IMAGINE 2013 software.[5] ERDAS IMAGINE

[4] Google Earth Engine is an online platform providing cloud computing facilities for satellite data processing (https://explorer.earthengine.google.com).

[5] ERDAS IMAGINE is a desktop software that is primarily used for remote sensing data analysis. (https://hexagon.com/products/erdas-imagine). This study used the ERDAS IMAGINE 2013 version of the software.

was used for development of the training sites,[6] signature evaluation and validation of results for both basins.

Spectral signatures were developed for each land cover type, from training site polygons at representative sample sites obtained from ground truth data collected during the field surveys and Google Earth images. Multiple signatures were developed for each land cover type to account for the variations in vegetation structure and density. Some additional subcategories were also defined to account for the variability within each vegetation type. These subcategories were later merged to form the final land cover categories defined earlier. The classification of agricultural areas into irrigated and rainfed areas was done using a different method, which is explained in the section *Classification of Irrigated Areas*. The distinction between irrigated and rainfed areas was not done when developing signatures.

Transformed Divergence (Swain and Davis 1978) was used as a statistical measure to evaluate the signature separability. The transformed divergence gives an exponentially decreasing weight to increasing distances between the signatures (Jensen 1996). The scale of the divergence values can range from 0 to 2,000. As a rule, if the result is less than 1,700, the separation is poor. The training sets were iteratively refined to achieve an acceptable level of separability between the signatures. The final set of training sites were exported to Google Earth Engine using the Fusion Tables[7] platform.

The selected Landsat 8 spectral bands (bands 2 to 7 and band 10), and the mean, standard deviation and two change layers derived from seasonal spectral indices were stacked together to define the base input dataset for the classification. The classification results were visually compared with Google Earth imagery using ERDAS IMAGINE. Manual editing techniques were used to refine the outputs wherever necessary. The manual editing was particularly useful in correcting misclassifications between water bodies and wetlands.

Land Cover Classification for the Early Time Period

The early time period for UGRRB was 1994-1995 and for UARB, it was the year 2000. The classification methods used were different for the two basins.

Table 1. Landsat images used for the land use and land cover classification of UGRRB and UAB.[a, b]

Landsat scene (path/row)	Early period	Late period	Cropping season
	Upper Great Ruaha River Basin (UGRRB)		
	Landsat 5 TM	Landsat 8 OLI and TIRS	
168/66	October 10, 1994	September 18, 2015	Pre-sowing
		May 16, 2016	Full crops
	June 23, 1995	July 3, 2016	Post-harvest
169/65	June 14, 1995	**June 23, 2016**	Post-harvest
169/66	August 14, 1994	September 9, 2015	Pre-sowing
	February 6, 1995	**May 6, 2016**	Full crops
	June 30, 1995	July 9, 2016	Post-harvest
	Upper Awash River Basin (UARB)		
	Landsat 7 ETM+	Landsat 8 OLI and TIRS	
168/54	February 5, 2000	March 10, 2015	Pre-sowing
		October 20, 2015	Full crops
	December 5, 2000	**December 23, 2015**	Post-harvest
169/54	March 15, 2000	January 28, 2015	Pre-sowing
		May 20, 2015	Growing
	November 26, 2000	**December 30, 2015**	Post-harvest

Notes:

[a] The dates in **bold** represent the primary images used for the classification (see section *Land Cover Classification for the Late Time Period*).

[b] Landsat images have a spatial resolution of 30 m (see Appendix).

[6] Training sites are known areas marked on the satellite image to develop a statistical characterization based on the pixel values for each potential output class.

[7] Fusion Tables is a data visualization web application to gather, visualize and share data tables (https://support.google.com/fusiontables/answer/2571232?hl=en).

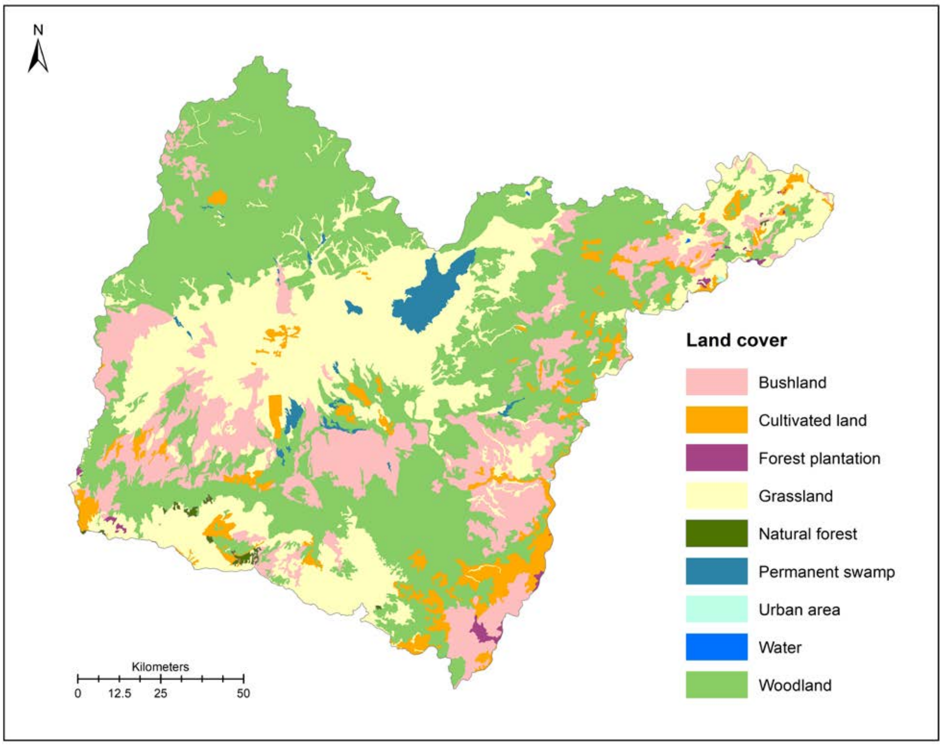

Figure 6. Land cover map from previous work on UGRRB in 1994.
Source: Prepared by the Institute of Resource Assessment (IRA), Tanzania.
Note: The land cover classes shown on the map are those used by IRA.

For UARB, land cover mapping for the year 2000 was performed through the method described in the section *Land Cover Classification for the Late Time Period*. Landsat ETM+ images were used for the classification. Due to cloud cover, only two season's images were available for the analysis (Table 1). The image for December 5, 2000, was selected as the primary image for classification of the Landsat scene 168/54 and the image from November 26, 2000, was selected for the Landsat scene 169/54. The BUI and the mean and standard deviation of NDVI and NDMI were derived and appended to the multi-spectral bands of the selected primary images to form the base dataset for the classification. Signature development, evaluation and classification procedures were followed as described in the section *Land Cover Classification for the Late Time Period*.

For UGRRB, as mentioned earlier, the map of 1994 prepared by IRA was used as a base map for the 1994-1995 classification (Figure 6). The base map was developed from the Landsat TM image of August 14, 1994, using unsupervised classification techniques. A visual comparison between this map and the satellite data used to develop it, showed that the heterogeneous land cover at finer scale in many areas is presented after significant generalization of the classification output. It was noted that many small or fragmented patches of agricultural areas were removed due to the generalization process. The grassland and bushland classes were similarly affected. As a classification using a single date imagery, the base map prepared by IRA was not capturing the variability in wetland extent over the seasons. In this study, the classification for 1995 was done by retaining the complex heterogeneity of the land cover at fine scale following the supervised classification methods used for the 2015 mapping.

Classification for the 1995 map was done using multi-season Landsat 5 TM images (Table 1). The primary images of each Landsat scene used for the analysis are as follows:

- 168/66: June 23, 1995
- 169/66: June 30, 1995

Based on the visual exploration, it was decided that the areas covered by the scene 169/65 did not need to be modified further. The additional variables based on the spectral indices were developed and the input layer stack for the classification was developed as described in the section *Land Cover Classification for the Late Time Period*. Neither ground truth information nor high-resolution images from Google Earth were available for the year 1995. Hence, training sites for classification were developed through visual interpretation of Landsat images.

Similar to the approach followed for the 2015 classification, the signatures were evaluated and refined using ERDAS IMAGINE and later exported to Google Earth Engine using Fusion Tables to perform the classification using Random Forest Classifier. All the Landsat 5 bands and the measures derived from multi-season spectral indices were used as the base dataset for classification.

The classification outputs were used to modify the land use map of 1994 and produce the final land cover map for further analysis.

Classification of Irrigated Areas

The irrigated and rainfed areas were not distinguishable through the initial classification using multi-spectral data and spectral indices, and the supervised classification. In UGRRB, irrigation mainly occurs in the wet season (Villholth et al. 2013). Therefore, classification techniques using temporal information, principally temporal variations in vegetation and moisture indices, were not suitable. Figure 7 illustrates the seasonal growth pattern, in terms of NDVI, of irrigated and rainfed areas along with the temporal rainfall distribution at two representative locations in UGRRB. The NDVI and rainfall profiles were derived from a time series of Moderate Resolution Imaging Spectroradiometer (MODIS) 16-day NDVI data (250 m resolution) and Climate Hazards group InfraRed Precipitation with Stations (CHIRPS) rainfall images (about 5 km resolution) for the same period. The trends shown in Figure 7 were developed by time series of a single pixel from each of the sites. As evident in Figure 7, there are no significant differences between the temporal growth pattern of irrigated and rainfed crops. However, the peak NDVI values are marginally higher in the irrigated areas.

Since the initial multi-spectral classification methods and temporal differentiation techniques were not successful in the classification of irrigated and rainfed crops, the temporal distribution of various spectral indices for irrigated and rainfed areas were explored in more detail. A set of 20 sample locations in all the irrigated and rainfed areas was selected from a subset of the UGRRB ground truth dataset, which included a variety of crops (irrigated and rainfed). Pixel values from all the spectral index layers, such as NDVI, MSAVI and NDMI derived for the initial classification, were explored. Additionally, the seasonal mean, seasonal standard deviation and the seasonal difference values for each variable were also explored. It was observed that the mean NDVI and mean NDMI are the two variables offering a marginal, but relatively consistent, differentiation among these variables (Figure 8). Both mean NDVI and mean NDMI were higher (not statistically tested) in irrigated areas compared to rainfed areas. NDVI and NDMI values have been successfully used in several studies to map the irrigated areas (Chance et al. 2017; Sharma et al. 2018). These indices are used in various ways – either separately or together with other potential information layers – based on the characteristics of the study area.

The irrigated and rainfed areas were differentiated by developing suitable thresholds for these two variables applicable for the entire basin. For UARB, thresholds were developed based on a set of 25 sample locations selected from the available ground truth data.

Accuracy Assessment

An accuracy assessment of the classification performed was carried out for the late time period (2015-2016) for both basins. This was done using a subset of the ground truth data and a set of stratified random validation points generated for the underrepresented categories in the ground truth surveys using Google Earth images.

For UGRRB, there were no GPS data with samples from wetlands, water bodies and forest plantations. Also, bushland and natural forest were underrepresented. Random points were generated for these classes to supplement the ground truth dataset. The actual land use types at the randomly generated locations were determined using Google Earth images. The final dataset consisted of 189 points, with 136 points from the ground truth data and 53 randomly generated locations. The comparison of reference data and classification results was carried out statistically using an error matrix (Story and Congalton 1986). The error matrix was used to estimate the user's accuracy, producer's accuracy and the overall accuracy of the map. User's accuracy is an estimate of the proportion of correctly classified pixels in the map and the producer's accuracy is the proportion of correctly classified reference points.

For UARB, the accuracy assessment was carried out in two steps due to the nature of the available reference data. Because the available GPS coordinates from the ground truth dataset from the Ministry of Agriculture contain only information on the irrigated agriculture class, accuracy of the rainfed class could not be determined. Also, the status of irrigation cannot be conclusively determined based on the Google Earth images. Therefore, for the initial step, the irrigated and rainfed classes were combined to form a single agriculture class.

First, a set of 224 validation points were generated using a stratified random technique, with a minimum of 30 locations in each class. Actual land use types at these locations were identified using Google Earth Engine. The comparison of reference data and classification results was carried out statistically using an error matrix as done for UGRRB.

Second, accuracy of the irrigated agriculture class was evaluated separately using the secondary ground truth data provided by Ministry of Agriculture. In this step, the accuracy assessment was carried out only for the irrigated agriculture class.

It was not possible to carry out the accuracy assessment for the early time period classification, because neither ground truth data nor high resolution images were available for that period. Quality assurance for this period was performed qualitatively for UGRRB by visually comparing the output with the satellite images and the available secondary map provided in Figure 6.

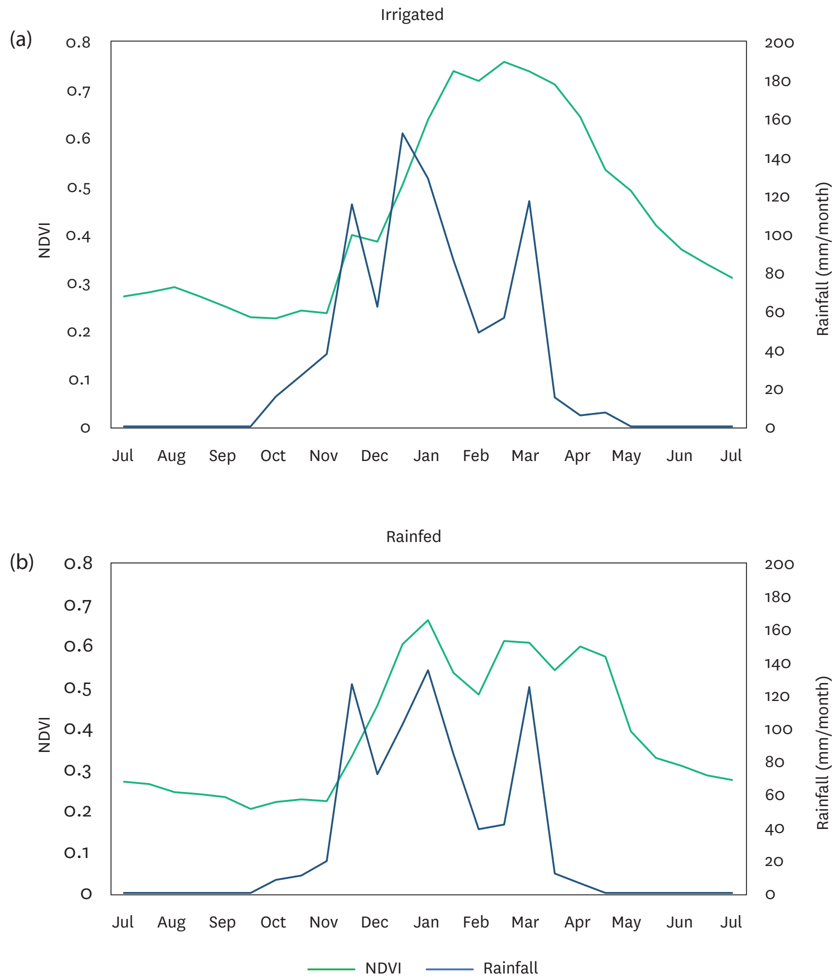

Figure 7. Annual variation in NDVI and rainfall for (a) irrigated, and (b) rainfed areas at two representative locations in UGRRB.

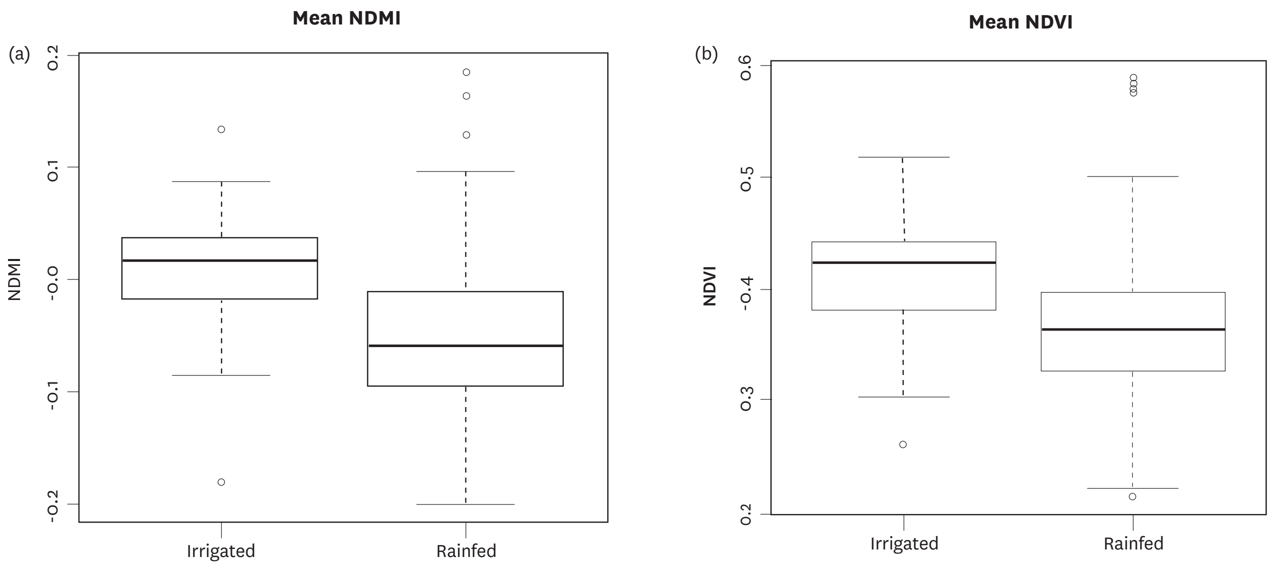

Figure 8. (a) Mean NDMI, and (b) Mean NDVI for irrigated and rainfed areas in UGRRB ($n_{irrigated}$ = 10; $n_{rainfed}$ = 10).

Analyzing Land Cover Change

A post-classification land cover change analysis was carried out to assess the changes that occurred between the two time periods for both basins using the final land cover maps. Various aspects of land cover change were explored by computing measures such as the net change in the area of each land cover type and the transition from one class to another. Detailed analysis was carried out to quantify the gains and losses in each land use category.

Results

Upper Great Ruaha River Basin

Land Cover Characteristics

Land cover maps developed for UGRRB through the classification process are shown in Figure 9. The land area covered by each category, estimated from the land cover maps, is provided in Table 2.

Table 2 shows that the basin is dominated by natural ecosystems, with agriculture accounting for 14.7% and 24.6% of the basin area in 1994-1995 and 2015-2016, respectively. Forest plantation and human settlement areas occupy less than 1% in both periods. Agriculture is mostly rainfed. The irrigated area covered 12.2% of the agricultural areas in 1994-1995 and 17.3% of the areas in 2015-2016.

Natural forest, woodland, bushland and grassland are the major natural vegetation classes found in UGRRB. Woodland occupies the largest area in the catchment with 47.6% in 1994-1995 and 44.1% in 2015-2016. Bushland also occupies a significantly large area with 22.4% in 1994-1995 and 18.9% in 2015-2016.

The basin has large wetland areas occupying 86,676 ha (4.2%) in 1994-1995 and 76,793 ha (3.7%) in 2015-2016. Kashaigili et al. (2006a) noticed that there is a significant difference in the area of vegetated wetlands between the wet and dry season, because the extent of inundated areas increases during the wet season. As the waterlogged areas decrease during the dry season, the extent of herbaceous vegetation and grasses increases. The multi-season images used in this study enable capturing the maximum seasonal extent of the wetland to a great extent. However, the maximum extent of the wetland during the peak rainy season can vary significantly from year to year depending on the seasonal rainfall. Annual rainfall estimated from the CHIRPS rainfall dataset is 1,019 mm in 1994 and 800 mm in 2015, partially explaining the differences in the extent of wetlands. The extent of water bodies was estimated as 282 ha in 1994-1995, but only 112 ha in 2015-2016.

Table 2. Area (absolute and relative) of different land cover types in UGRRB for the periods 1994-1995 and 2015-2016.

No.	Land cover class	Area in 1994-1995		Area in 2015-2016	
		Hectares	%	Hectares	%
1	Irrigated agriculture	37,311	1.79	88,704	4.26
2	Rainfed agriculture	268,749	12.91	423,095	20.32
3	Grassland	221,881	10.66	162,574	7.81
4	Bushland	465,763	22.37	393,428	18.89
5	Woodland	990,499	47.57	918,829	44.12
6	Natural forest	6,068	0.29	7,356	0.35
7	Forest plantation	3,693	0.18	4,107	0.20
8	Human settlement	1,460	0.07	7,384	0.35
9	Wetland	86,676	4.16	76,793	3.69
10	Water body	282	<0.01	112	<0.01
	Total	2,082,382	100.00%	2,082,382	100.00%

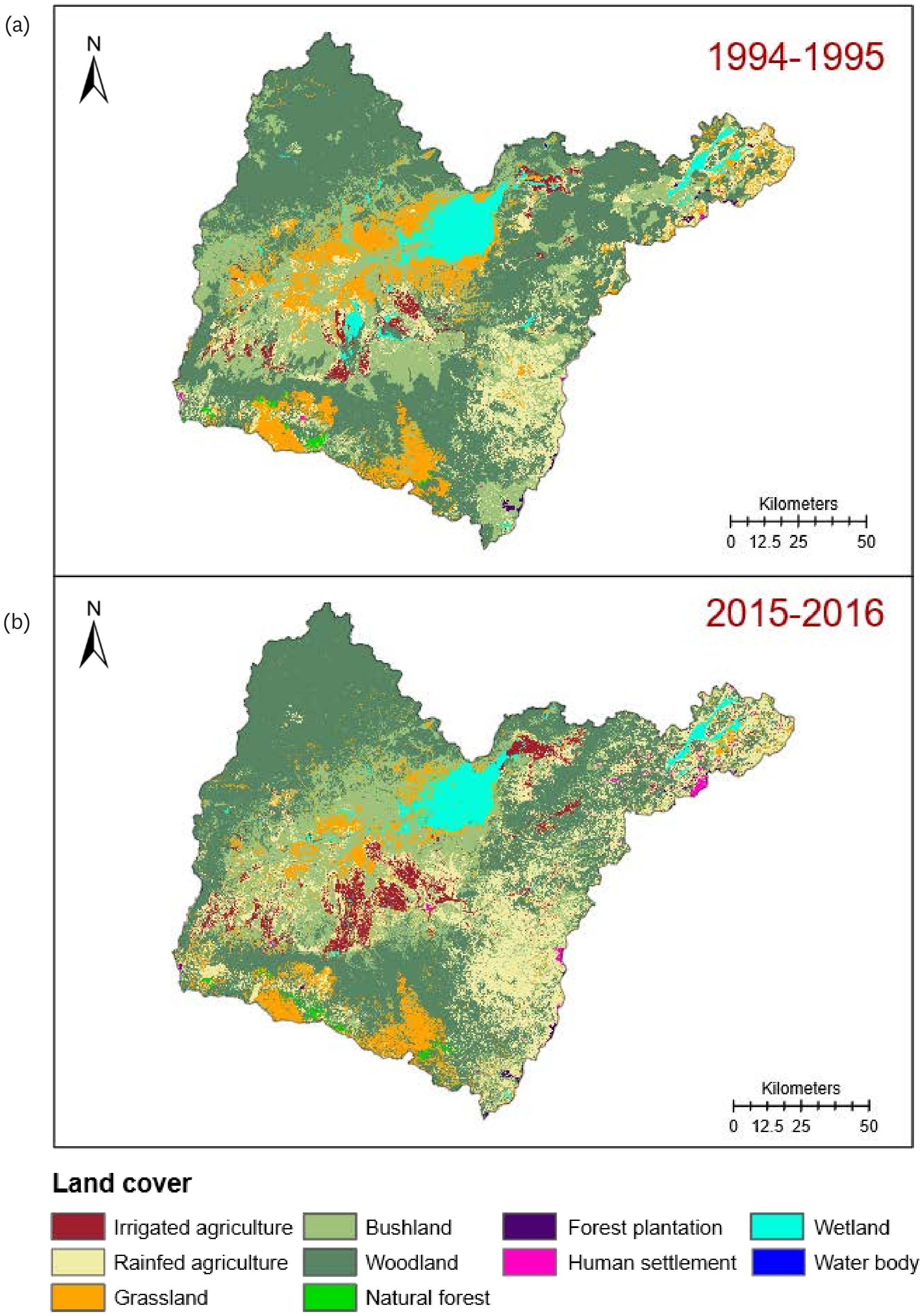

Figure 9. Land cover maps of UGRRB for the periods (a) 1994-1995, and (b) 2015-2016.

Accuracy Assessment

The results of the accuracy assessment of the UGRRB classification for 2015-2016 are provided in the form of an error matrix in Table 3. Overall, the results show a good agreement (77.8%) between the output and reference data. Both irrigated and rainfed agriculture classes show good accuracies, with producer accuracies of 73.7% and 76.3%, respectively, and user accuracies of 87.5% and 84.9%, respectively. Natural vegetation types such as grassland, bushland and woodland show relatively lower producer accuracies of 60%, 82.4% and 63.2%, respectively, and lower user accuracies of 64.3%, 63.6% and 63.2%, respectively. The error matrix shows the potential misclassification of rainfed agriculture, which would have resulted in an overestimation of these categories. The nature of fragmented small-scale agriculture adjacent to the grassland, bushland and woodland areas could be a reason for this. All the random sample reference points collected from the wetland and water body classes were correctly classified, and this resulted in a 100% producer accuracy for these classes.

However, the error matrix shows that there are other categories misclassified as wetland and water body, which resulted in user accuracies of 87% and 80%, respectively. This indicates that there is a small overestimation of wetland and water body classes due to the misclassification of other categories as these classes, most importantly irrigated agriculture and bushland. Human settlements in the area generally have a mix of trees and small agricultural plots. Additionally, most houses in smaller settlements are built with natural roofing material. This has affected the success of identifying smaller settlements, but the identification of larger settlements and small towns were relatively successful. The human settlement class has both user and producer accuracies of 71.4%.

Land Cover Change

Various aspects of the land cover change dynamics in UGRRB were explored through a post-classification change analysis using the final land cover maps. The map in Figure 10 shows the distribution of areas that underwent and did not undergo land cover change during the study period. The map shows that a substantial part of the catchment experienced changes during this 20-year period (from 1994-1995 to 2015-2016). It is estimated that 619,874 ha or 29.8% of the catchment underwent changes. There is a tendency for more intensive changes towards the center, i.e., the lowlands, of the basin.

Table 4 and Figure 11 provide an overview of the changes in each land cover type. The decrease (loss), increase (gain) and the net change in area of each land cover type are summarized in Table 4. Interestingly, most land cover types show substantial changes in both directions (Figure 11). Details of the loss and gain or changes to each land cover class are described in the next section *Land Cover Transitions*.

The data show that both agriculture classes (irrigated and rainfed) had a net increase in the total area. However, both categories also experienced a decrease or conversion to other categories in some areas. Rainfed agriculture shows the highest net increase among all categories with 154,346 ha, which is a 57.4% increase from the situation in 1995. Irrigated agriculture also had a substantial increase during this period. The total irrigated area more than doubled (from 37,311 to 88,704 ha, Table 2), with a net increase of 51,393 ha (137.7%). The built-up areas (human settlement class) in the basin have increased from 1,460 to 7,384 ha showing a fourfold net increase (405.8%) in the total area of that category.

Grassland, bushland and woodland are the major natural land cover types in the basin. Of these, grassland and bushland show a major net reduction (26.7% and 15.5%) in the total extent, while woodland shows a smaller net reduction of 7.2%. There is a fairly large extent of wetland areas within the basin, covering almost 76,793 ha in 2016. During the study period, the total wetland area had decreased by 11.4%, but as stated earlier, it is not clear whether this is a long-term trend or a natural seasonal variation.

Land Cover Transitions

Tables 5 and 6 report the transition of various land cover types in UGRRB from 1994-1995 to 2015-2016 in absolute (Table 5) and relative (Table 6) numbers. The change matrix provided in these tables illustrates the detailed conversion between the various land cover types present in the basin. The values along the rows (except the gray boxes, indicating areas of land cover that did not change) indicate how much of the earlier extent (1994-1995) of each land cover type was converted to other land cover types over the study period. In other words, these values indicate the losses in the area of each land cover type. Conversely, the values along the columns show the extent of land cover type that was added from other land cover types in the late time period (2015-2016).

There was a significant increase in the irrigated and rainfed areas from 1994-1995 to 2015-2016 (Table 4). Table 5 shows that these additions were mainly from woodland and bushland areas. During this period, 100,546 ha of woodland and 69,681 ha of bushland were converted to rainfed agriculture. This is 10.15% and 14.96% of woodland and bushland areas, respectively, in 1994-1995 (Table 6). Similarly, 12,595 ha of grassland also got converted to rainfed agriculture. Irrigated areas showed similar trends of conversion from woodland, bushland and grassland areas. In addition to these, 15,428 ha of rainfed areas were also converted to irrigated areas. While the overall agricultural extent shows an increase, it may also be noted that in some areas, previous agricultural (rainfed) land was converted to grassland (9,252 ha) and bushland (7,271 ha) (Table 5).

Table 3. Error matrix of the accuracy assessment of the UGRRB classification for 2015-2016, showing the comparison of the classification results and the reference points (n=189) and the user and producer accuracies.

	Land cover class	*Reference data*											
		Irrigated agriculture	Rainfed agriculture	Grassland	Bushland	Woodland	Natural forest	Forest plantation	Human settlement	Wetland	Water body	Total	User accuracy (%)
Classified data	Irrigated agriculture	14	2									16	87.50
	Rainfed agriculture	1	45	1		4	1		1			53	84.91
	Grassland	1	4	9								14	64.29
	Bushland	1	3	2	14	2						22	63.64
	Woodland		4	3		12						19	63.16
	Natural forest						12	1				13	92.31
	Forest plantation		1				2	8	1			12	66.67
	Human settlement	1				1			5			7	71.43
	Wetland				2		1			20		23	86.96
	Water body	1			1						8	10	80.00
	Total	19	59	15	17	19	16	9	7	20	8	189	
	Producer accuracy (%)	73.68	76.27	60.00	82.35	63.16	75.00	88.89	71.43	100.00	100.00		

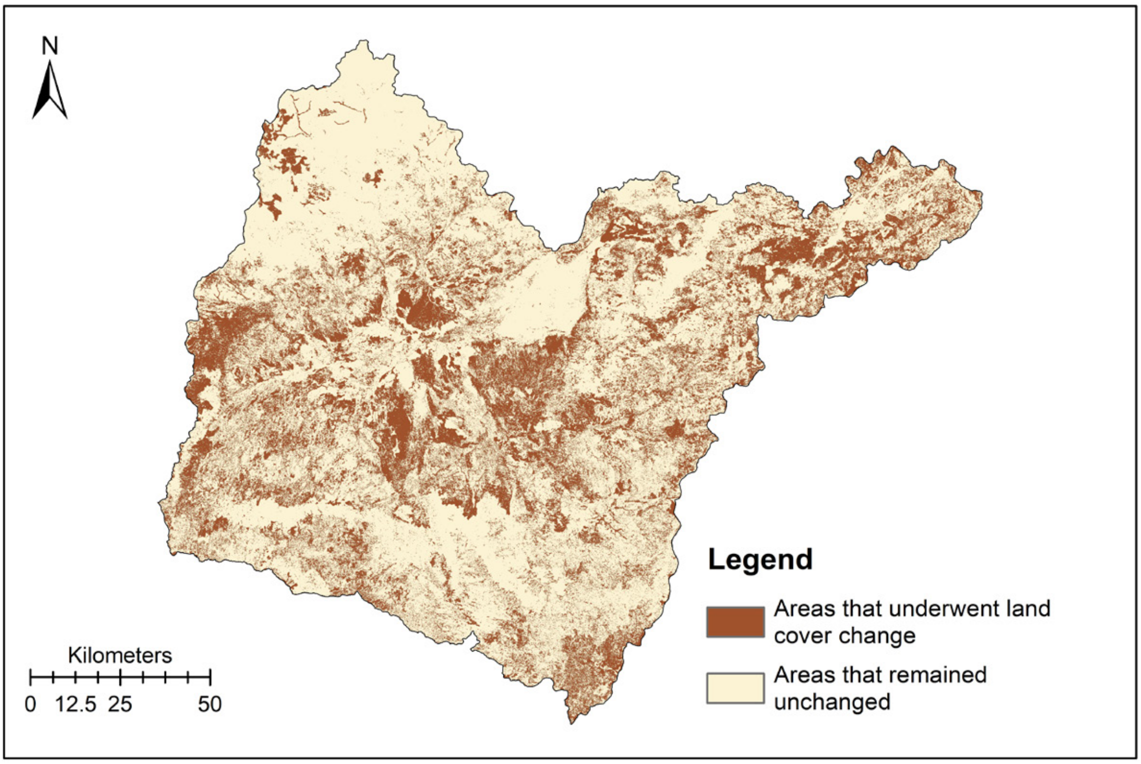

Figure 10. Map of areas that underwent land cover change and areas that remained unchanged in UGRRB from 1994-1995 to 2015-2016.

In line with this, the major natural land cover types showed a decrease in their overall area (Table 4). The reduction in bushland and grassland is quite significant at 15.5% and 26.7%, respectively (Table 4). Although, there was a substantial conversion of grassland to rainfed agriculture (12,595 ha), the largest conversion from grassland was to bushland (81,248 ha), corresponding to 36.6% of grassland. A similar trend in the conversion of bushland to grassland and woodland can be observed.

Another major land cover type of the basin is wetlands (4.16% in 1994-1995, Table 2). While ca. 84% of wetland areas remained unchanged during this period, irrigated agriculture was a major land use that encroached into wetland areas (7,687 ha or 8.9% of wetland area in 1994-1995).

Table 4. Net change (absolute and relative) in the area of different land cover types in UGRRB between 1994-1995 and 2015-2016.

No.	Land cover class	Change in area (ha)			Net change in area (%)[a]
		Loss	Gain	Net change	
1	Irrigated agriculture	5,187	56,580	51,393	137.74
2	Rainfed agriculture	36,131	190,477	154,346	57.43
3	Grassland	120,011	60,705	-59,306	-26.73
4	Bushland	225,396	153,061	-72,335	-15.53
5	Woodland	213,637	141,967	-71,670	-7.24
6	Natural forest	2,604	3,892	1,288	21.23
7	Forest plantation	2,249	2,663	414	11.21
8	Human settlement	692	6,616	5,924	405.75
9	Wetland	13,796	3,913	-9,883	-11.40
10	Water body	170	0	-170	-60.4

Note: [a] Change in area (%) is calculated with respect to the area of the land cover type in 1994-1995 (Table 2).

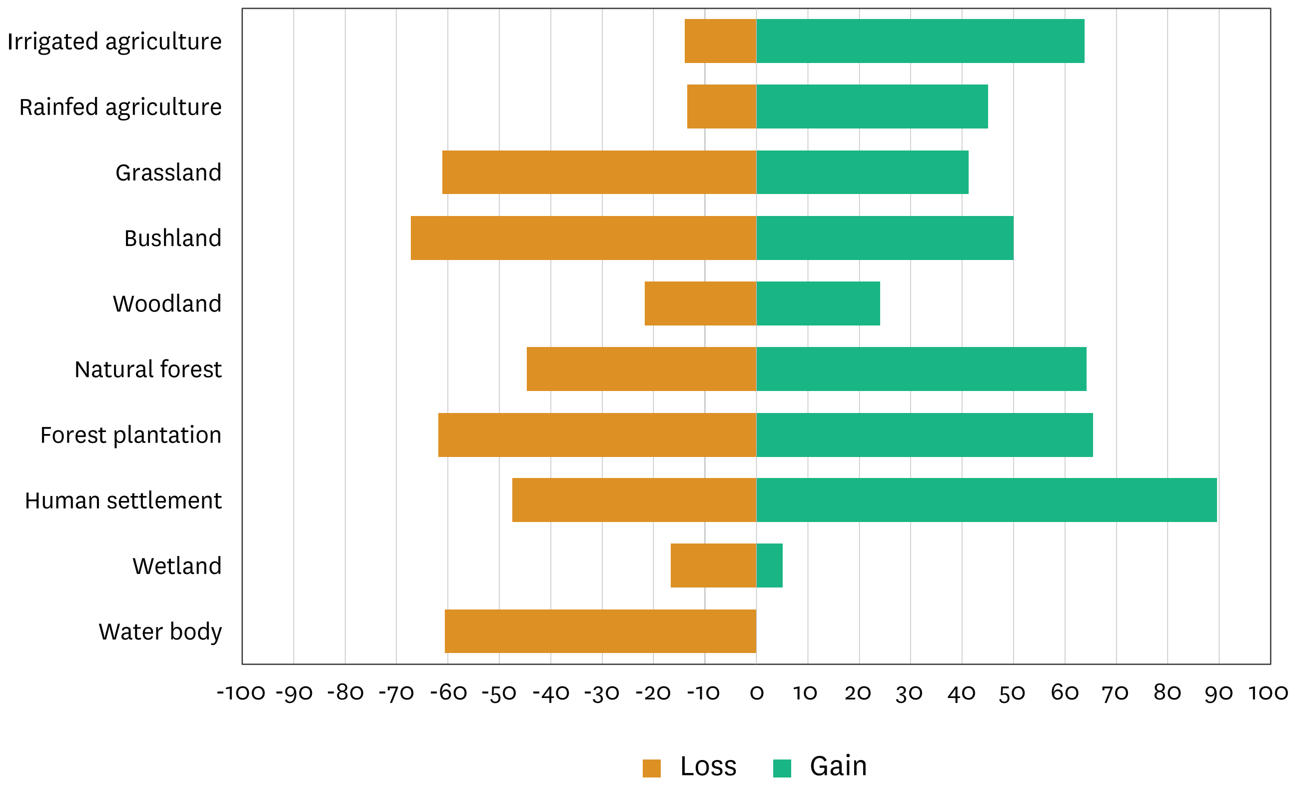

Figure 11. Gains and losses of different land cover types in UGRRB during the periods 1994-1995 and 2015-2016.
Note: The percentage of losses is calculated using the area of the initial period (1994-1995) as the base and the percentage of gains is calculated using the area of the later period (2015-2016) as the base.

Table 5. Area of land cover transitions for each land cover class in UGRRB from 1994-1995 to 2015-2016.

	Land cover class	Area in 2015-2016 (ha)										
		Irrigated agriculture	Rainfed agriculture	Grassland	Bushland	Woodland	Natural forest	Forest plantation	Human settlement	Wetland	Water body	Grand total
Area in 1994-1995 (ha)	Irrigated agriculture	32,124	4,370	204	563	0	0	16	13	21	0	37,311
	Rainfed agriculture	15,428	232,618	9,252	7,271	215	0	538	3,178	249	0	268,749
	Grassland	1,879	12,595	101,869	81,248	18,851	197	378	1,390	3,474	0	221,881
	Bushland	12,471	69,681	23,346	240,367	118,184	0	644	1,070	0	0	465,763
	Woodland	19,067	100,546	26,094	63,080	776,862	3,586	394	870	0	0	990,499
	Natural forest	3	147	211	38	2,205	3,464	0	0	0	0	6,068
	Forest plantation	44	800	31	178	1,041	62	1,444	93	0	0	3,693
	Human settlement	0	0	0	0	0	0	692	768	0	0	1,460
	Wetland	7,687	2,338	1,567	683	1,471	47	1	2	72,880	0	86,676
	Water body	1	0	0	0	0	0	0	0	169	112	282
	Grand total	88,704	423,095	162,574	393,428	918,829	7,356	4,107	7,384	76,793	112	2,082,382

Table 6. Percentage of land cover transitions in UGRRB from 1994-1995 to 2015-2016.[a]

	Land cover class	Area in 2015-2016 (%)									
		Irrigated agriculture	Rainfed agriculture	Grassland	Bushland	Woodland	Natural forest	Forest plantation	Human settlement	Wetland	Water body
Area in 1994-1995 (%)	Irrigated agriculture	86.10	11.71	0.55	1.51	0.00	0.00	0.04	0.03	0.06	0.00
	Rainfed agriculture	5.74	86.56	3.44	2.71	0.08	0.00	0.20	1.18	0.09	0.00
	Grassland	0.85	5.68	45.91	36.62	8.50	0.09	0.17	0.63	1.57	0.00
	Bushland	2.68	14.96	5.01	51.61	25.37	0.00	0.14	0.23	0.00	0.00
	Woodland	1.92	10.15	2.63	6.37	78.43	0.36	0.04	0.09	0.00	0.00
	Natural forest	0.05	2.42	3.48	0.63	36.34	57.09	0.00	0.00	0.00	0.00
	Forest plantation	1.19	21.66	0.84	4.82	28.19	1.68	39.10	2.52	0.00	0.00
	Human settlement	0.00	0.00	0.00	0.00	0.00	0.00	47.40	52.60	0.00	0.00
	Wetland	8.87	2.70	1.81	0.79	1.70	0.05	0.00	0.00	84.08	0.00
	Water body	0.41	0.00	0.00	0.00	0.00	0.00	0.00	0.00	59.93	39.72

Note: [a] The percentage is calculated by considering the area in 1994-1995 as a base.

Upper Awash River Basin

Land Cover Characteristics

The land cover maps for UARB for the years 2000 and 2015, developed through the classification process, are shown in Figure 12. The area of each land cover type and the percentage of each type within the basin for 2000 and 2015 are provided in Table 7.

Land cover of the basin was classified into eight categories in both years. The results show that agriculture is the dominant land cover type in the UARB, covering 65.9% of the basin in 2000 and 80.6% in 2015. Within the agricultural areas, irrigated agriculture occupied 1.1% in 2000 and 2.0% in 2015. Area-wise, built-up areas (human settlements) occupied a relatively small but significantly increasing part of the basin – 1.6% in 2000 and 4.5% in 2015 (Table 7). Land cover maps (Figure 12) show that much of these built-up areas are concentrated around Addis Ababa in the northern part of the basin. Agricultural and built-up areas, the two non-natural land cover types found in the basin, show an increase between 2000 and 2015.

Bushland, grassland and forest are the major natural vegetation types in the basin. Among these, bushland covered the largest area in 2000 (22.5%), followed by grassland (5.3%) and forest (3.9%). In 2015, bushland, grassland and forest covered 4.7%, 6.3% and 2.9%, respectively.

Water bodies and wetlands are also found in various parts of the basin. The combined area occupied by these land cover types is less than 1% of the basin in both years.

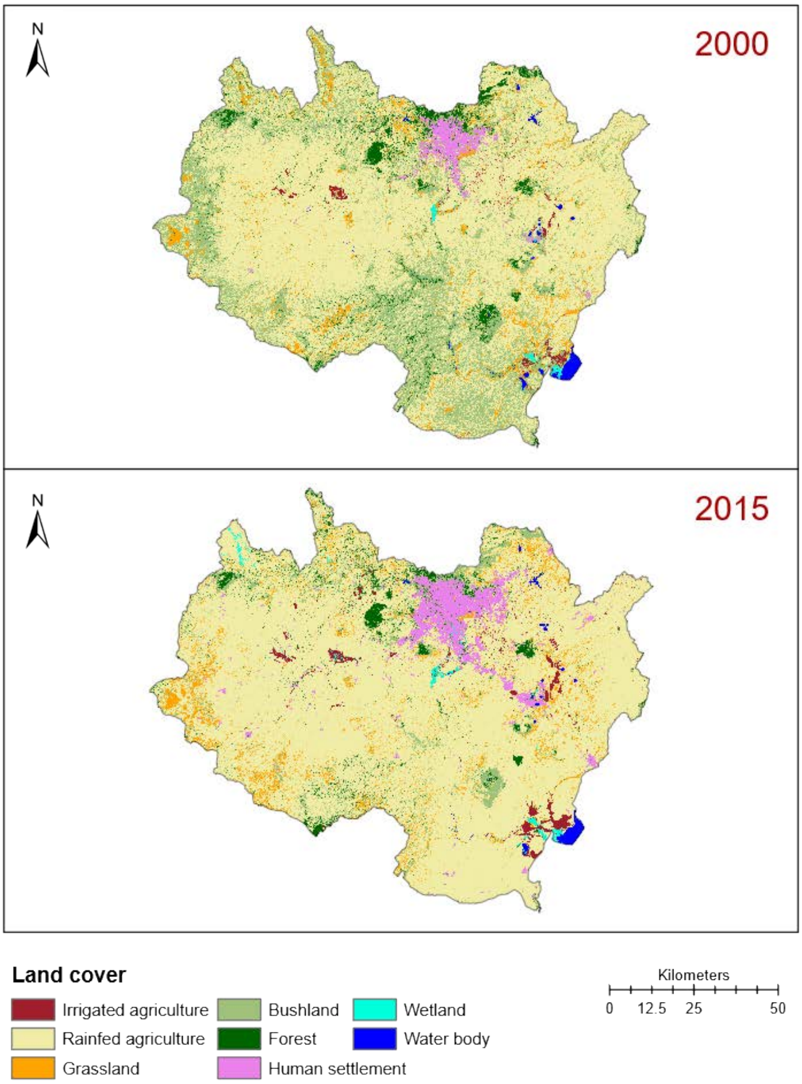

Figure 12. Land cover maps for UARB for (a) 2000, and (b) 2015.

Table 7. Area (absolute and relative) of different land cover types in UARB for 2000 and 2015.

No.	Land cover class	Area in 2000		Area in 2015	
		Hectares	%	Hectares	%
1	Irrigated agriculture	7,443	0.70	16,936	1.58
2	Rainfed agriculture	697,301	65.19	844,827	78.99
3	Grassland	57,103	5.34	67,761	6.34
4	Bushland	241,083	22.54	50,498	4.72
5	Forest	41,418	3.87	31,213	2.92
6	Human settlement	17,202	1.61	48,072	4.49
7	Wetland	2,257	0.21	4,953	0.46
8	Water body	5,774	0.54	5,321	0.50
	Total	1,069,581	100.00	1,069,581	100.00

Accuracy Assessment

The results of the accuracy assessment for the UARB classification of 2015 are provided in the form of an error matrix in Table 8. The analysis shows an overall accuracy of 81.3%. Highest reliabilities were observed for wetland and human settlement, where the producer accuracy was more than 90%. The agriculture and forest classes also have a high accuracy with both measures (user and producer accuracies) being more than 80%. The separate accuracy assessment, which was carried out only for the irrigated area within the agricultural areas, shows a 73.9% accuracy for the irrigated agriculture classification (cf. section *Accuracy Assessment* under the section *Land Cover Classification and Change Analysis*). The omission error is highest for grassland with a producer accuracy of only 63.2%. This could be due to the insignificant spectral differences between grassland and fallow agricultural land or the misclassification of grassland to bushland or forest due to the presence of scattered trees or bushes in grasslands, and this would have caused an underestimation of the grassland area.

Land Cover Change

The overall distribution of land cover change in the basin during the study period is visualized in Figure 13. Although the changes are widespread, the distribution and intensity of the changes are not uniform across the landscape, though there is a tendency for more intensive changes toward the boundaries, i.e., the highlands, of the basin. It is estimated that 364,464 ha or 34.1% of the basin witnessed land cover change in some form over the 15-year period (2000-2015).

Table 8. Error matrix of the accuracy assessment for the UARB classification of 2015, showing the comparison of classification results and the reference points (n=224), and the user and producer accuracies.

Land cover class		*Reference data*								User accuracy (%)
		Agriculture	Grassland	Bushland	Forest	Human settlement	Wetland	Water body	Total	
Classified data	Agriculture	29	2		2	2			35	82.86
	Grassland	4	24	6					34	70.59
	Bushland	3	4	23	1	1	1		33	69.70
	Forest		2	2	26				30	86.67
	Human settlement		3		1	28			32	87.50
	Wetland		3				23	4	30	76.67
	Water body						1	29	30	96.67
	Total	36	38	31	30	31	25	33	224	
Producer accuracy (%)		80.56	63.16	74.19	86.67	90.32	92.00	87.88		

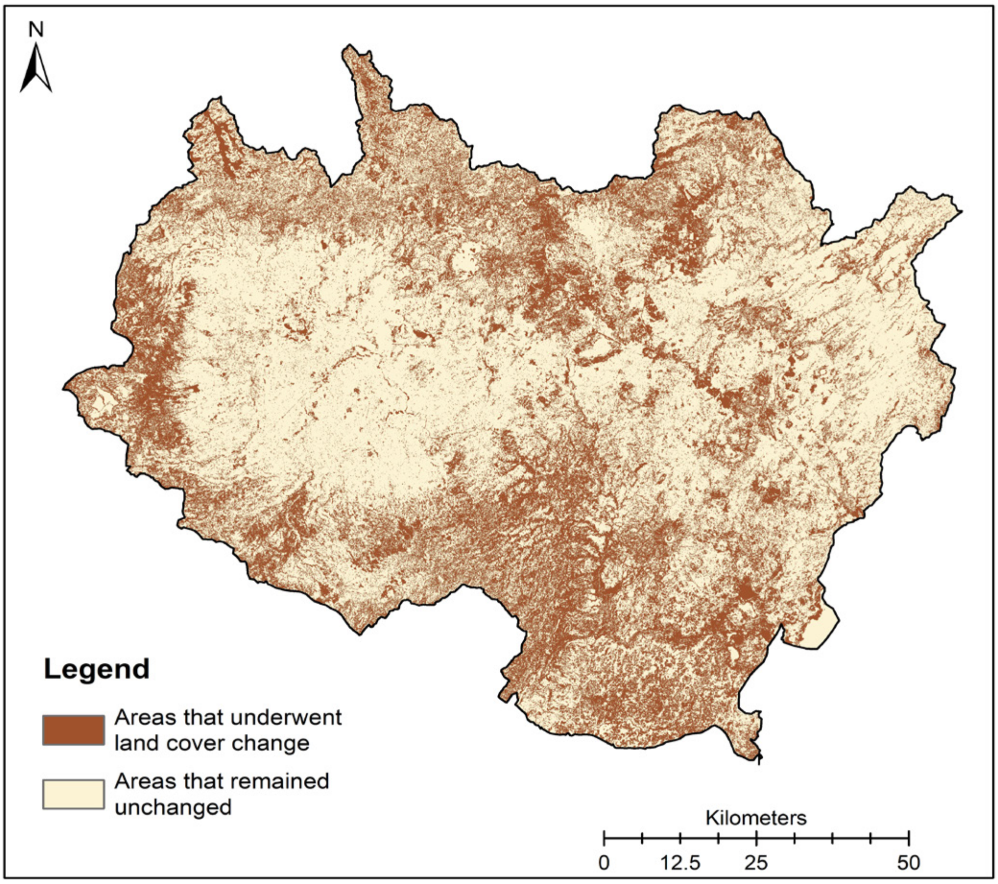

Figure 13. Map of the areas that underwent land cover change and areas that remained unchanged in UARB from 2000 to 2015.

Table 9 provides estimates of the net changes in each land cover type in the basin. Area-wise, bushland (-190,585 ha) and rainfed agriculture (147,526 ha) experienced the largest net changes. These changes amount to -79.1% and 21.2% of the earlier areas of bushland and rainfed agriculture, respectively. Percentagewise, human settlements showed the largest gain (179.5%, corresponding to a net increase of 30,870 ha), followed by irrigated agriculture (127.5%, corresponding to a net increase of 9,493 ha).

The area estimations in Table 9 show that most land cover types underwent changes in both directions, i.e., increase in area in some locations and a reduction in area in other locations. Along with Table 9, Figure 14 illustrates the nature of the relative changes in the basin. Except for built-up areas (human settlements), all categories show a bidirectional pattern of change. Table 9 shows that some of the categories, although the net change is low, have substantial counterbalancing loss and gain in different areas. Grassland (loss of 45,370 ha, gain of 56,028 ha) and forest (loss of 32,765 ha, gain of 22,560 ha) are two such categories that underwent substantial changes. Except for human settlement and agricultural areas, most land cover types display a strong bidirectional pattern of loss and gain during the study period (Figure 14).

Land Cover Transitions

Tables 10 and 11 and Figure 15 summarize and illustrate the transition of each land cover class from 2000 to 2015. Much of the areas that were covered by human settlements, and irrigated and rainfed agriculture in 2000 remained the same in 2015 by retaining 100%, and 90.8% and 89.6%, respectively (Table 11). However, classes such as grassland, bushland and forest showed substantial changes by retaining only 20.6%, 12.4% and 20.9%, respectively, of the earlier areas.

Although the original agricultural areas in 2000 remained mostly unchanged, the irrigated agriculture class had substantial gains from other classes, with an addition of 10,176 ha (Table 9). Much of this addition was contributed from rainfed agriculture (5,910 ha), followed by bushland (2,923 ha) (Table 10). The net increase in rainfed agriculture (21.2%, Table 9), on the other hand, was primarily from bushland (170,481 ha) and grassland (36,048 ha). Similarly, a significant portion of the rainfed agricultural area was converted to urban areas (18,720 ha). It can also be seen that 15,419 ha of the rainfed area were converted to forest, which indicates the proliferation of tree plantations in agricultural areas. However, the largest change in rainfed area is the conversion to grassland (31,953 ha).

Table 9. Net change (absolute and relative) in the area of different land cover types in UARB between 2000 and 2015.

No.	Land cover class	Change in area (ha)			Net change in area (%)[a]
		Loss	Gain	Net change	
1	Irrigated agriculture	683	10,176	9,493	127.53
2	Rainfed agriculture	72,373	219,899	147,526	21.16
3	Grassland	45,370	56,028	10,658	18.66
4	Bushland	211,167	20,582	-190,585	-79.05
5	Forest	32,765	22,560	-10,205	-24.64
6	Human settlement	0	30,870	30,870	179.46
7	Wetland	715	3,411	2,696	119.45
8	Water body	1,391	938	-453	-7.85

Note: [a] Change in area (%) is calculated based on the area of the land cover type in 2000 (Table 7).

Among the natural land cover, bushland was occupying the largest share with 22.5% of the entire basin in 2000 (Table 7), and it underwent the largest net change during this period (-190,585 ha) (Table 9). Only 12.4% of the earlier bushland area remained unchanged (Table 11). While 70.7% of earlier bushland was converted to rainfed agriculture, bushland was also converted to grassland (9.1%) and human settlements (3.3%) (Table 11). At the same time, large areas under forest cover (15,896 ha) were converted to bushland. These changes have resulted in a net overall reduction of bushland from 22.5% of the basin in 2000 to just 4.7% in 2015 (Table 7). While major parts of the grassland and forest classes were converted to rainfed agriculture, these categories also partially gained from a reverse change from the same categories elsewhere. In aggregate, there were only marginal changes in the total areas of grassland (5.3% to 6.3%) and forest (3.9 to 2.9%) (Table 7). However, there was a clear location shift evident in these categories because only ca. 20% of the earlier areas remained unchanged (Table 11).

A noticeable feature of the land cover change in UARB is the expansion of human settlement areas. The analysis shows that while almost the entire area occupied by this category in 2000 remained unchanged, substantial areas of other land cover types were converted and added to built-up areas (human settlements). As a result, there was an almost threefold increase in human settlement areas in this period (1.6 to 4.5%, Table 7). Much of this expansion was at the expense of rainfed agricultural areas (18,720 ha) and bushlands (8,034 ha) (Table 10).

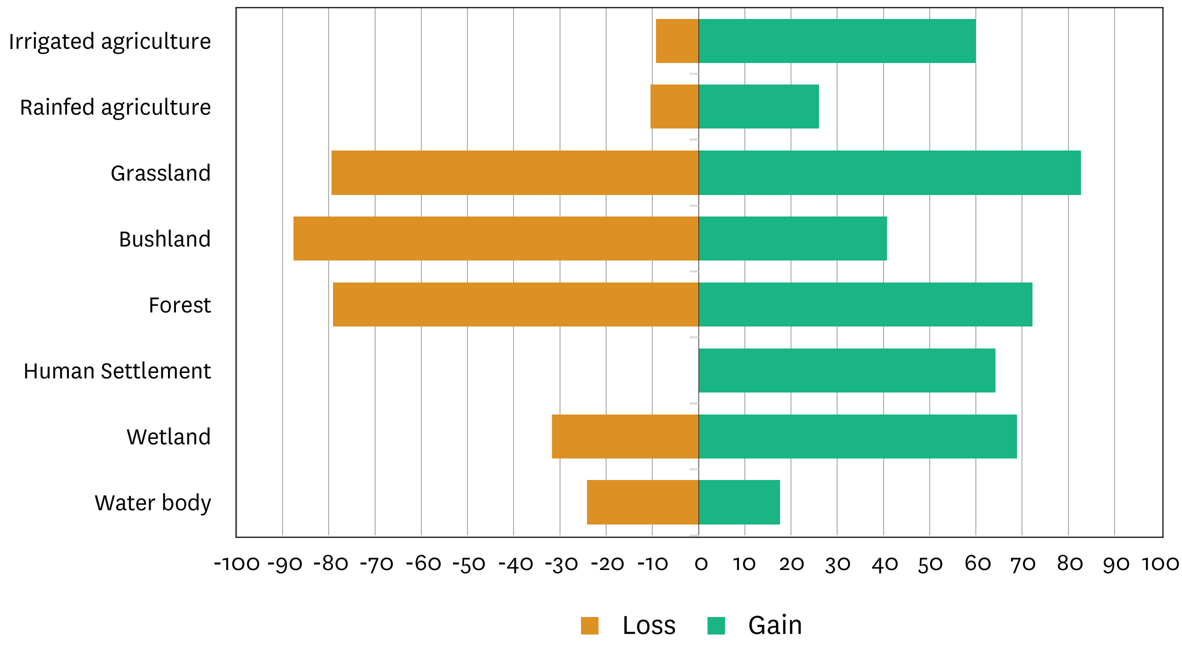

Figure 14. Gains and losses of different land cover types in UARB between 2000 and 2015.
Note: The percentage of losses is calculated using the area of the initial period (2000) as the base and the percentage of gains is calculated using the area of the later period (2015) as a base.

Table 10. Area of land cover transitions for each land cover type in UARB from 2000 to 2015.

Land cover class		Area in 2015 (ha)								
		Irrigated agriculture	Rainfed agriculture	Grassland	Bushland	Forest	Human settlement	Wetland	Water body	Grand total
Area in 2000 (ha)	Irrigated agriculture	6,760	0	185	0	76	282	86	54	7,443
	Rainfed agriculture	5,910	624,928	31,953	0	15,419	18,720	327	44	697,301
	Grassland	653	36,048	11,733	4,613	275	1,998	1,472	311	57,103
	Bushland	2,923	170,481	21,922	29,916	6,719	8,034	901	187	241,083
	Forest	403	12,571	1,884	15,896	8,653	1,659	310	42	41,418
	Human settlement	0	0	0	0	0	17,202	0	0	17,202
	Wetland	119	212	31	10	33	10	1,542	300	2,257
	Water body	168	587	53	63	38	167	315	4,383	5,774
	Grand total	16,936	844,827	67,761	50,498	31,213	48,072	4,953	5,321	1,069,581

Table 11. Percentage of land cover transitions in UARB from 2000 to 2015.[a]

Land cover class		Area in 2015 (%)							
		Irrigated agriculture	Rainfed agriculture	Grassland	Bushland	Forest	Human settlement	Wetland	Water body
Area in 2000 (%)	Irrigated agriculture	90.82	0.00	2.49	0.00	1.02	3.79	1.16	0.73
	Rainfed agriculture	0.85	89.62	4.58	0.00	2.21	2.68	0.05	0.01
	Grassland	1.14	63.13	20.55	8.08	0.48	3.50	2.58	0.54
	Bushland	1.21	70.71	9.09	12.41	2.79	3.33	0.37	0.08
	Forest	0.97	30.35	4.55	38.38	20.89	4.01	0.75	0.10
	Human settlement	0.00	0.00	0.00	0.00	0.00	100.00	0.00	0.00
	Wetland	5.27	9.39	1.37	0.44	1.46	0.44	68.32	13.29
	Water body	2.91	10.17	0.92	1.09	0.66	2.89	5.46	75.91

Note: [a] The percentage is calculated by considering the area in 2000 as a base.

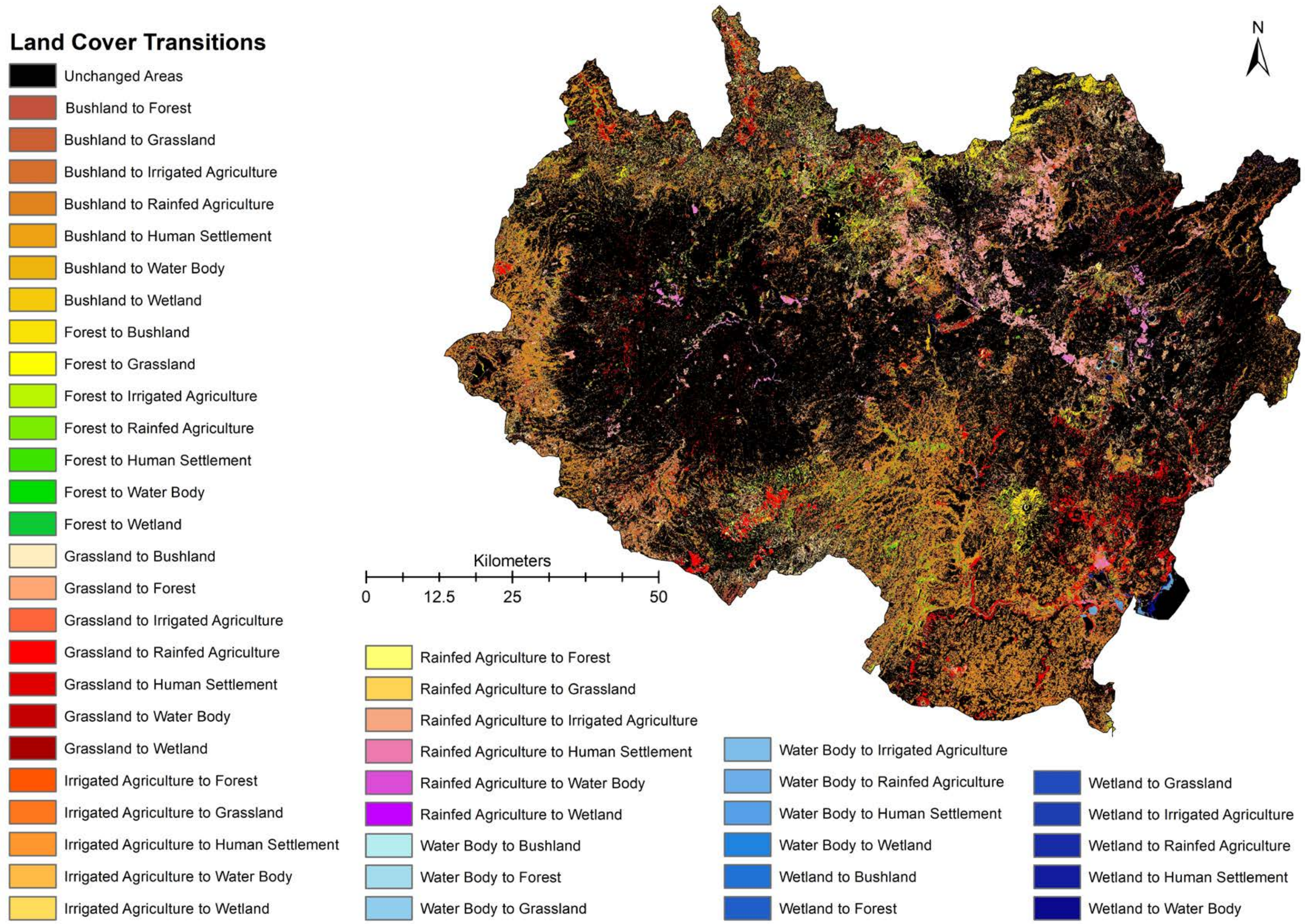

Figure 15. Land cover transitions in UARB from 2000 to 2015, indicating all combinations of land cover type changes that occurred during the period.

Discussion

Land cover changes in diverse tropical agrarian landscapes are complex in nature. This study quantifies and analyzes the patterns of change in two upper basins in Ethiopia and Tanzania using satellite images from two periods, approximately two decades apart. The results of the analysis demonstrate the varying nature of the patterns of change. Apart from quantifying the changes in each land cover category, the study quantifies the transitions between different land cover types and provides information about the dominant characteristics of the change. The results of the land cover mapping were partially validated using field information collected through ground truth datasets. The ground truth data collection and validation were carried out only for the late time period (2015-2016) as there were no suitable datasets available for the early time periods (1994-1995 for UGRRB and 2000 for UARB) for validation. While there are no defined standards, generally, an overall accuracy of 80 to 85% and no single land cover class having an accuracy lower than 60% are considered acceptable for thematic land cover classification. However, it is often difficult to achieve this in highly complex landscapes such as UGRRB. The overall accuracy of the classification for 2015-2016 was 77.8% for UGRRB and 81.3% for UARB; the accuracy of individual land cover classes for both basins is within the acceptable limit, indicating that the classification is reasonably successful in capturing the land cover patterns. However, the inability to validate the results of the early time period due to the lack of field data is a shortcoming of this study.

The results show that 29.8% and 34.1% areas in UGRRB and UARB, respectively, underwent some form of land cover change during the study period. Despite the satisfactory validation results, there is a certain amount of misclassification between the land cover classes. Misclassification between spectrally similar land cover categories is the key source of uncertainty in thematic classification using remote sensing data. Land cover classes such as fallow agricultural land and grassland, rainfed and irrigated agriculture, woodland and natural forest, etc., are potential pairs of misclassification. While the results illustrate the overall trends, incorporating intermediate time periods in the analysis would have provided more insights about the trajectory of change, especially if there were any shifts or variations in the rate of changes. The following sections discuss the results in each basin.

Land Cover Changes in the Upper Great Ruaha River Basin

The major human-dominated land cover types in UGRRB are agriculture and human settlements. Both these land cover types showed substantial growth in their extent between 1994-1995 and 2015-2016. The net change in the area of irrigated agriculture was 138% and that of rainfed agriculture was 57% (Table 4). The human settlement areas had an increase of 406%. From the transition table (Table 5) and Figure 16, it is evident that while the expansion of agricultural areas was mainly in the previously natural land cover areas such as woodland and bushland, the growth of human settlements was mostly from the conversion of rainfed agricultural areas. As defined in the classification scheme, the human settlements include built-up structures for residential/commercial purposes, which may be interspersed with small farmlands or other fragmented land uses. The loss of human settlement areas to forest plantations indicates the conversion of small farmlands and tree clusters within settlements to monoculture tree plantations.

Major parts of UGRRB are covered by natural land cover types. The major natural land cover classes include grassland, bushland and woodland, which covered 80.6% in 1994-1995 and 70.8% in 2015-2016. All these land cover types showed a considerable reduction in net area during the study period from 1994-1995 to 2015-2016.

However, the transition tables (Tables 5 and 6) indicate that a substantial area of these three categories (grassland, bushland and woodland) exchanged between each other. These exchanges show that while there is an overall reduction in these areas, large parts of the natural land cover in the basin are showing a regeneration of vegetation. Table 12 is an extract from the land cover transition table (Table 5). The conversion to denser vegetated areas is shown in green whereas the conversion to less vegetated areas is shown in light brown. A pair-wise comparison between each of these categories illustrates a shift towards denser vegetation types. The change indicated by the values in the green cells is considerably higher than those in the light brown cells. Together, the conversion to denser vegetation in these three categories is almost twice the conversion to less vegetated areas. These three categories covered almost 80% of the basin in 1995. Further, similar changes can also be observed in natural forest. Overall, it can be stated that excluding the conversion to agriculture and human settlements, the natural land cover types in the basin predominantly exhibit a shift towards greener or more woody vegetation.

This increase in vegetation cover may be linked to specific local factors or broader-scale regional drivers of change.

The spatial distribution of the greening trend indicates that a significant part of it occurs in the alluvial plains (fans) around the wetland region (Figure 17). Past studies have reported a drying up of the Great Ruaha River during the dry season and occurring since 1993 for many years, presumably due to expansion of irrigation (Kashaigili et al. 2006a, 2009); some studies link earlier degradation of the wetland ecosystem to unregulated cattle grazing (SMUWC 2001b; Kihwele et al. 2012).

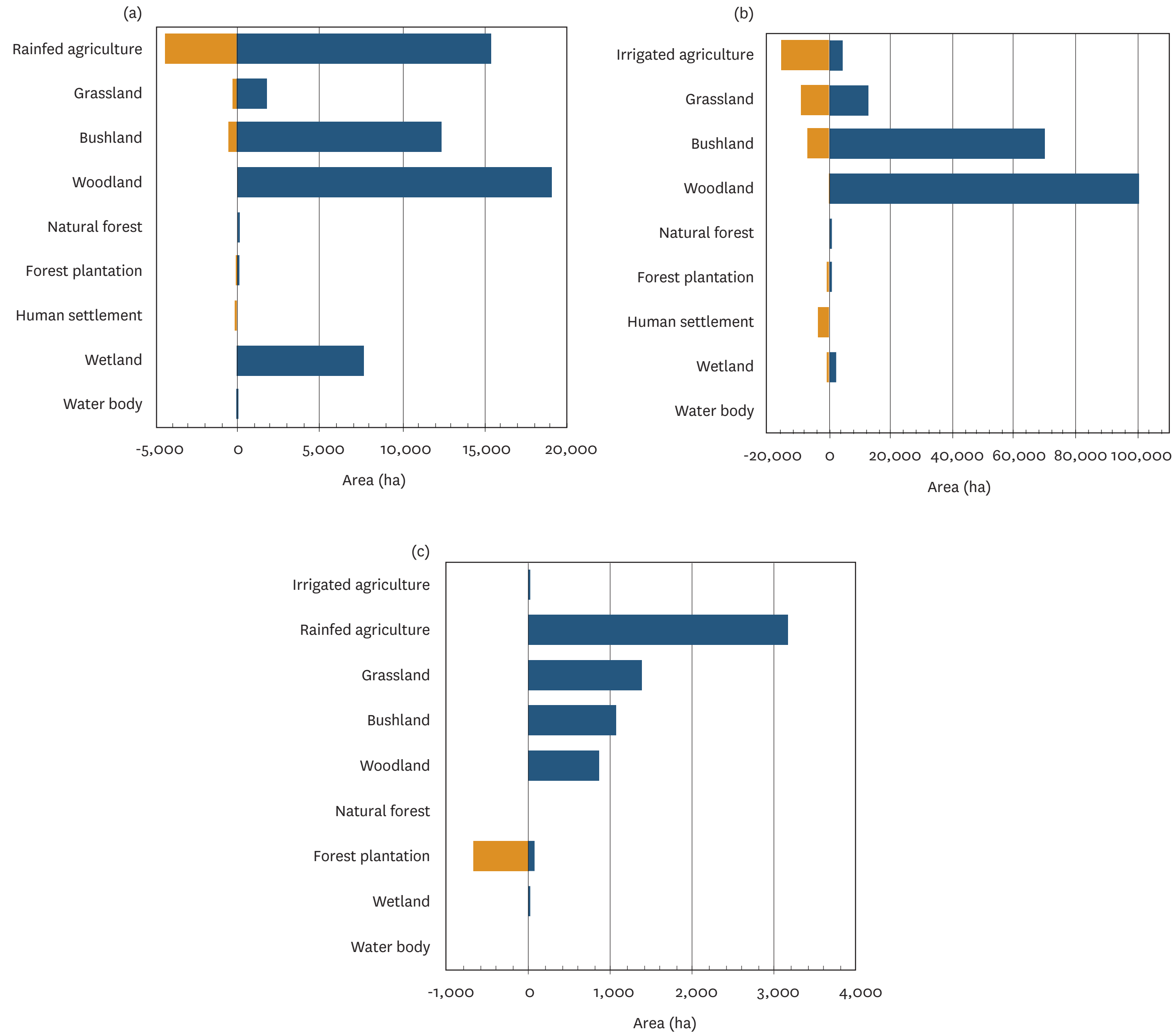

Figure 16. Contributions of various land cover types to net change in the areas of (a) irrigated agriculture, (b) rainfed agriculture, and (c) human settlement in UGRRB between 1994-1995 and 2015-2016.
Note: The x-axes are scaled differently.

Table 12. Conversion of land cover types to more densely vegetated categories in UGRRB between 1994-1995 and 2015-2016.

	Land cover class	Area 2015-2016 (ha)		
		Grassland	Bushland	Woodland
Area 1994-1995 (ha)	Grassland		81,248	18,851
	Bushland	23,346		118,184
	Woodland	26,094	63,080	

Note: The conversion to denser vegetated areas is shown in green whereas the conversion to less vegetated areas is shown in light brown.

Overgrazing has a direct detrimental impact on vegetation cover by trampling and burning of vegetation by shepherds. In an attempt to restore the dry season flow and wetland ecosystem, the Government of Tanzania expanded the Ruaha National Park (RNP) to include the Usangu wetland in 2008 and restricted cattle grazing (Kihwele et al. 2018). Figure 17 indicates that the major portion of the areas exhibiting an increase in greening is within the newly added areas of RNP. The increasing greening close to the wetland region may have links to the recovery of wetlands and reduction in grazing due to the expansion of the RNP and removal of cattle.

Similar to the increase in greenness in the natural vegetation, agriculture in the basin also witnesses an intensification and expansion of irrigated areas. There has been an increase of 137.7% (51,393 ha) in the irrigated area within the basin during the study period (Table 4). The expansion of irrigation is mostly occurring in the southern fans of the wetland region (Figure 17). As shown in Figure 17, much of the greening trend (both agriculture and natural vegetation) is within the alluvial plains. The trend of increase in natural vegetation cover is also witnessed in areas away from the alluvial plains.

While there may be local factors influencing such changes, it must be noted that similar patterns have been observed in other regions of Africa. A general increase in greenness or vegetation productivity in several semi-arid areas in Africa after the 1980s has been reported by studies based on Earth observation data (Huber et al. 2011; Hickler et al. 2005; Eklundh and Olsson 2003). These studies, based on different datasets and different methods, also report significant regional variations in this observed trend, including vegetation decline in many areas. There could be several explanations for these trends, including recovery from drought, precipitation changes, and a possible effect of a tropical carbon sink and/or local factors such as resource use affecting the vegetation cover. Local factors such as afforestation, irrigation development or a shift in the dependence on the natural ecosystems may also result in such changes. However, it was reported that even seemingly similar increases in greenness or vegetation cover in different areas may have widely different explanations (Fensholt et al. 2012). The bidirectional nature of changes observed in natural vegetation types in UGRRB during the study period concur with the reported trends of vegetation change in several other parts of Africa. Much of the increase in vegetation cover in UGRRB is occurring in areas in or adjacent to the alluvial plains, which were included in RNP in 2008 (Figure 17), indicating that the reported local factors such as expansion of the protected area and restriction in grazing could be drivers of change.

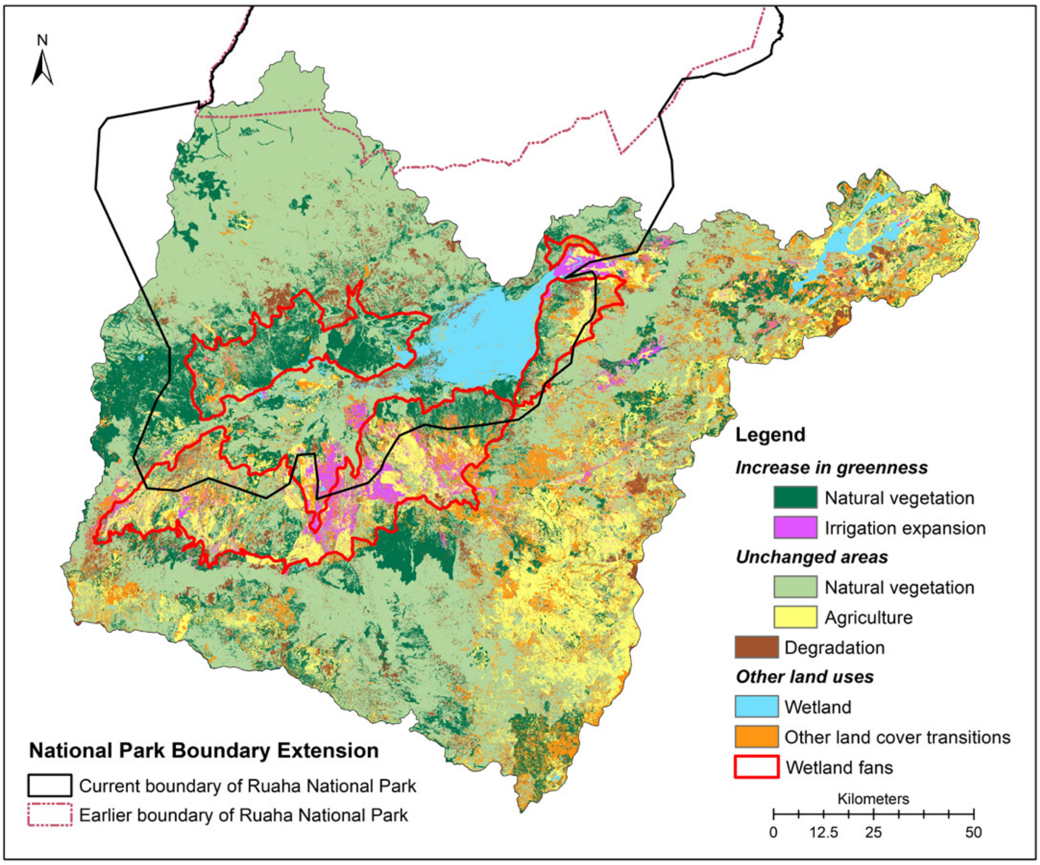

Figure 17. Vegetation cover in UGRRB. Areas showing an increase in or recovery of vegetation cover and irrigation expansion in UGRRB.

Land Cover Changes in the Upper Awash River Basin and Comparison with the Upper Great Ruaha River Basin

Agriculture is the largest land cover type in UARB and has undergone a major expansion between 2000 and 2015. Agricultural areas covered almost 65.9% of the basin in 2000 and increased to 80.6% of the basin by 2015 (Table 7). Figure 18 illustrates the land cover types converted to irrigated and rainfed agriculture during this period, based on Table 10. While a major part of the expansion of irrigated agriculture was due to conversion of bushland and rainfed agriculture, the expansion in rainfed agriculture was mostly due to conversion of bushland.

There was a fourfold increase in human settlements in the basin during this period, from 17,202 ha in 2000 to 48,072 ha in 2015 (Table 7). Figure 18 shows that this expansion was mainly from the conversion of rainfed agricultural areas and to a lesser extent from bushland areas. Figure 12 illustrates the distributed expansion of agriculture and urbanization between 2000 and 2015. The dominant pattern emerging from this analysis is schematically shown in Figure 19. Comparing Figures 16 and 18, it is evident that many of the overall land cover transitions are similar for the two basins, illustrating a general trend across these landscapes that includes a transition of natural land (such as grassland, bushland and woodland/forests) first to rainfed agriculture and subsequently to irrigated agriculture, and then a transition of parts of agricultural areas (mostly rainfed) to human settlements (Figure 19). Some encroachment on wetlands was also seen, in the case of UGRRB. Human settlements and irrigated areas did not seem to be significantly transitioning back to other land cover types, presumably because of the significant and concentrated investments in associated infrastructure.

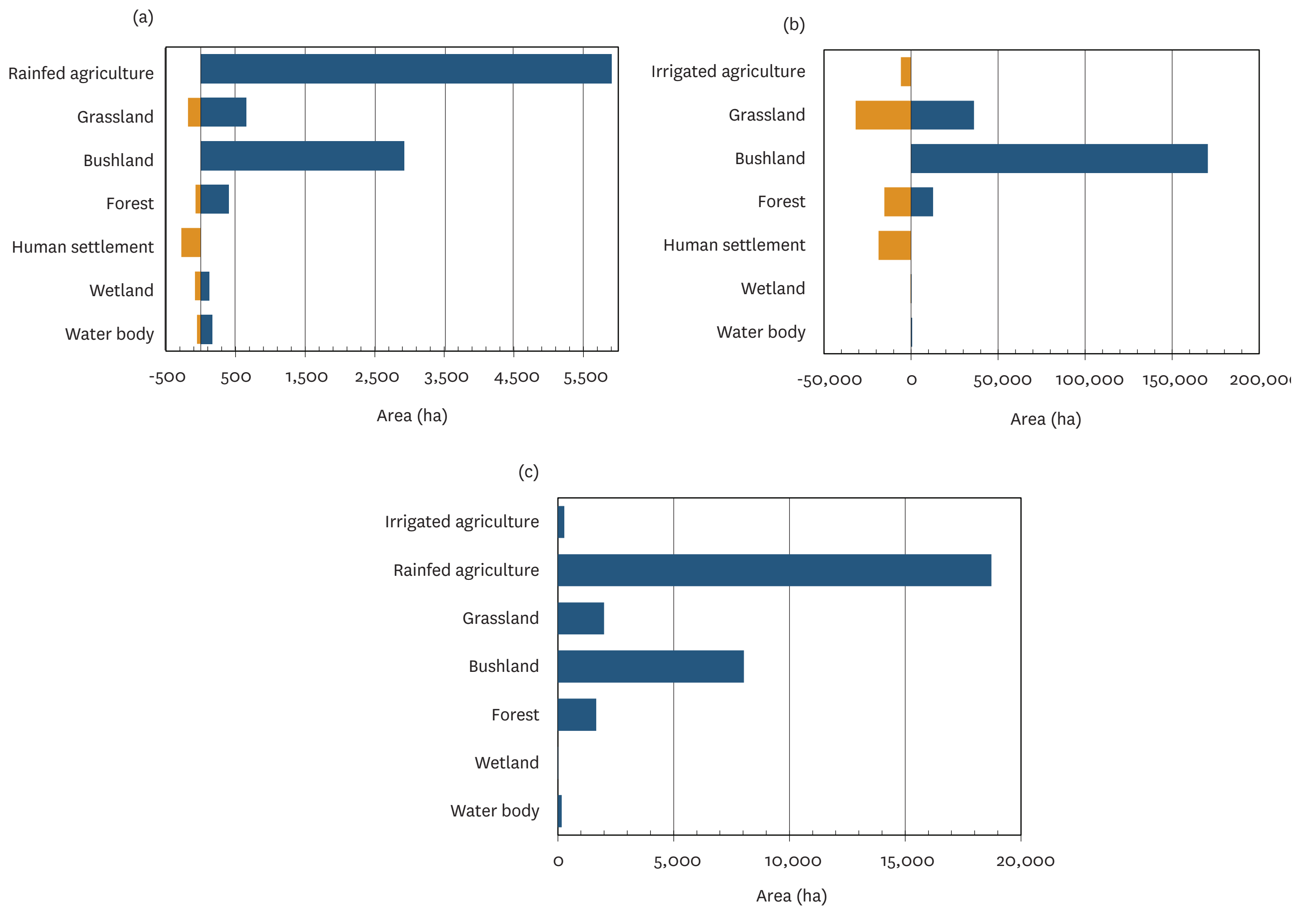

Figure 18. Contributions of various land cover types to net change in the areas of (a) irrigated agriculture, (b) rainfed agriculture, and (c) human settlement in UARB between 2000 and 2015.

Note: The x-axes are scaled differently.

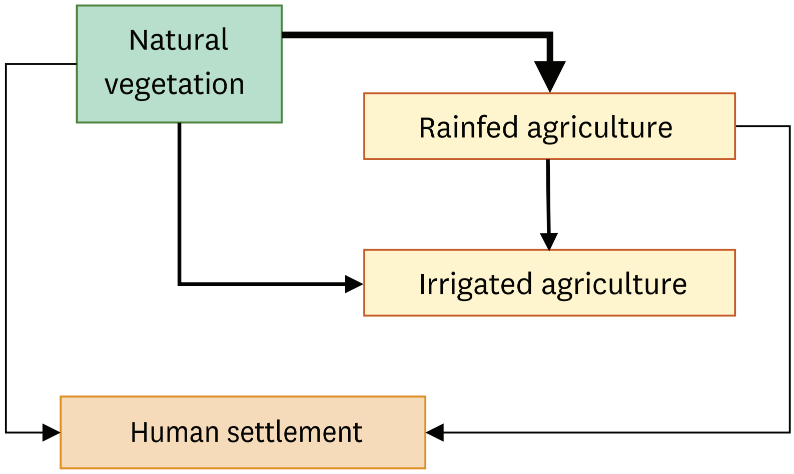

Figure 19. Generalized land cover change pathways in both UGRRB and UARB. The thickness of the lines indicates the strength of the trends.
Note: 'Natural vegetation' includes grassland, bushland and woodland/forest.

With nearly 80% of agricultural areas and 4.5% of human settlement areas (Table 7), the natural land cover in UARB is alarmingly low. The pattern of greening or shift to more woody vegetation types, as observed in UGRRB, is absent in UARB. If the trend shown in Figure 19 continues, the basin might lose the remaining natural land cover in the near future.

For UGRRB, the situation is somewhat different. Here, the agricultural areas and human settlement areas cover only 24.6% and 0.4%, respectively (Table 2), of the basin, while natural land cover types cover the remaining area. Therefore, the basin is under relatively less stress. However, it should be emphasized that the UGRRB encompasses a very critical ecosystem of wetlands, upstream of significant conservation areas and hydropower dam infrastructure (Villholth et al. 2013). In addition, the area has a relatively higher degree of irrigation development as of 2016 (17.3% of agricultural areas versus 2.0% in UARB), indicating relatively more intensive use of the water resources. However, irrigation is also picking up significantly in UARB, with a long-term average annual development rate of 8.5% in irrigated areas compared to 6.9% in UGRRB (Table 13).

Table 13. A comparison of relative changes in UGRRB and UARB. The rate of change was calculated based on the early time period.

Land cover class	Average annual rate of change	
	UGRRB	UARB
Irrigated agriculture	6.89%	8.50%
Rainfed agriculture	2.87%	1.41%
Grassland	-1.34%	1.24%
Bushland	-0.78%	-5.27%
Woodland	-0.36%	
Natural forest	1.06%	
Forest		-1.64%
Forest plantation	0.56%	
Human settlement	20.29%	11.96%
Wetland	-0.57%	7.96%
Water body	-3.01%	-0.52%

While the annual expansion rate of human settlements in UGRRB (20.3%) is higher than UARB (12.0%), it must be noted that the recent net change in the human settlement area in UGRRB (5,924 ha) is much less than UARB (30,870 ha) (Tables 4, 9 and 13). The higher rate of expansion is due to the fact that the human settlement area was marginal in the early time period, so even a small increase resulted in a higher expansion rate for the category. So, while the catchments may be seen as following a parallel trajectory, some significant differences are observed, i.e., irrigation development occurred relatively earlier in UGRRB, while urban development has been a more prominent feature of UARB, though irrigation development seems to be increasing currently.

Land cover patterns and transitions of a region could be significantly influenced by a combination of sociopolitical conditions, economic activities, demographic profiles, ecological characteristics, and biophysical factors such as climate, water resource availability, etc. Although identifying specific determinants of particular land cover changes occurring in these basins or their implications was beyond the scope of this study, it would be worth discussing some of the major aspects of the basins, which could have an impact on the observed patterns of changes. These characteristics were identified based on the analyses and conclusions reported by similar studies from the region.

Globally, food production and economic activities to support a growing population are major drivers of land cover change. The results indicate significant growth in human settlements and expansion of agricultural areas in both the basins. Population growth increases the demand for food, feed, fuelwood and infrastructure, and has been a major driver for intensifying natural resource use. Growth of industrial production and commercial trade is also likely to increase the requirement for land resources for constructing infrastructure. Ethiopia and Tanzania have been experiencing substantial population growth rates in recent decades, e.g., 2.5% and 2.9% in 2020, respectively.[8]

With the presence of the large urban agglomeration around Addis Ababa city, UARB has the largest concentration of urban population and industries in Ethiopia. A fairly good road network and direct access to the international maritime port of Djibouti, which is Ethiopia's main import/export outlet, provide better access to both domestic and international markets and promote commercial and industrial investment, production and trade in the region. The construction of the Ethio-Djibouti Railway (1897–1917), connecting Addis Ababa to Djibouti, which passes through the eastern part of the basin, has facilitated early development of commercial and industrial ventures in this region (Oqubay 2018).

Awash River Basin is one of the most intensively cultivated basins in Ethiopia since the introduction of modern agriculture (Berhe et al. 2013; Gedefaw et al. 2019). The growth of population, urban centers and industries in the basin also provides opportunities for large-scale commercial agriculture. The modern irrigation systems were introduced in Ethiopia in the 1950s, initially in the Awash Basin for growing commercial crops such as cotton, sugarcane and horticultural crops (Awulachew et al. 2007). Studies from elsewhere in Ethiopia reported population increase as one of the major reasons for the conversion of natural vegetation to agriculture in many areas of the country (Gashaw et al. 2017; Hassen and Assen 2018; Hurni et al. 2005). The shift from rainfed to irrigated agriculture in UARB also underlines the need for increasing food production.

Unlike UARB, UGRRB is not an economic-industrial hub promoting urbanization. Rather, ecosystem services provided by wetlands attracted pastoralists and farmers from elsewhere in the country to UGRRB in the 1980s and 1990s (Sosovele and Ngwale 2002; Kashaigili et al. 2006a), which was later restricted by the government (Walsh 2012). Sosovele and Ngwale (2002) have attributed the expansion of residential areas to population growth during this period. Kashaigili et al. (2006b) reported that population growth in UGRRB has led to the expansion of agriculture in areas with natural vegetation in the basin. Although modern agriculture and irrigation were introduced in the basin in the 1940s, major population growth was associated with the rapid expansion of irrigated areas after the 1970s (Kashaigili 2008).

Changes in vegetation cover can directly affect various hydrological processes such as runoff, infiltration, evapotranspiration, etc. In a previous study, Kashaigili et al. (2008) reported significant changes in the flow regime and its impact on the Usangu wetland in UGRRB due to the effects of deforestation and an increase in irrigated areas. Our study identified an increase in woody vegetation and green biomass in certain areas of the basin, which can be primarily attributed to the expansion of the RNP in 2008 and restrictions imposed by the government on cattle grazing (Kihwele et al. 2018). It would be worth exploring the impact of this increase in vegetation cover on dry season flow and restoration of Usangu wetland. Similarly, in UARB, Beyene et al. (2018) found that streamflow had increased during the wet season and reduced during the dry season, and surface runoff had increased, due to the conversion of natural vegetation to agriculture.

[8] Statista: https://www.statista.com/statistics/1227666/population-growth-rate-in-africa-by-country/#:~:text=All%20the%20African%20countries%20registered,three%20percent%20of%20growth%20each (accessed on February 20, 2022).

Changes in natural ecosystems may have negative consequences on the livelihoods of dependent communities. For example, conversion of grassland into other land uses would reduce the availability of fodder for livestock, which would further impact a series of livelihood activities prevalent in an agrarian society. In northwestern Ethiopia, a reduction in grassland led to a shortage of livestock, which further impacted farming activities such as plowing, transporting, manuring, etc., and reduced income from animal products (Zeleke and Hurni 2001). The drying up of the river and reduction of wetlands in UGRRB after 1993 (Kashaigili et al. 2006a), and again in 2013 and 2015 (Stears et al. 2018), presumably due to anthropogenic influences, had a profound impact on regional biodiversity, which was evident in the water stress and mortality rates of associated species in the downstream RNP (Kashaigili et al. 2006a).

Implications of Land Cover Change for Groundwater Resources

Significant land cover changes in UGRRB and UARB over the last decades, exacerbated by climate change, imply intensified land and water use, including groundwater. There is good evidence that groundwater is increasingly being developed to meet growing water needs for both urban and rural community water supplies and productive uses, such as irrigated agriculture (Worqlul et al. 2017; Villholth et al. 2013), as well as providing a buffer against droughts and climate change more generally in the basins (Birhanu et al. 2021; Hyandye 2019). In Addis Ababa, the relative use of groundwater for public water supply has increased from around 9% to more than 50% since the early 2000s (Healy et al. 2022). With more dependence on groundwater, the question naturally arises, how will land cover and water use changes likely affect groundwater resources and dependent ecosystems in these basins in the future.

From a qualitative assessment, and building on previous assessments, the following impacts on groundwater resources (recharge, storage and quality) are projected.

1. **Land cover change towards more rainfed agriculture**

   Rainfed agriculture underwent a large increase of 57% and 21% in UGRRB and UARB, respectively. If the original natural vegetation is more water consuming than agricultural crops (e.g., more deep-rooted vegetation like bushland or forest), this transition could lead to increased groundwater recharge and raised groundwater levels. This effect has been observed widely across the relatively flat Sahel (Favreau et al. 2009). On the other hand, groundwater recharge could be significantly impaired if land becomes degraded in the process (e.g., increased cultivation or livestock rearing and overgrazing on unstable or easily erodible hillslope areas). Land degradation is a real hazard in the Ethiopian highland context in the UARB, where erosion in upper catchments with higher slopes is a significant issue (Daba and You 2022). It is, therefore, important to protect land cover, especially in important recharge areas of major aquifers (e.g., through the use of exclosures, contour bunding and proper road construction [Mekuria et al. 2009]).

2. **Land cover change towards more urbanization**

The largest relative land cover change is conversion to larger human settlement/urban areas (increase of 406% and 180% in UGRRB and UARB, respectively). This change could imply a decrease in groundwater recharge, due to an increase in paved/impermeable surface areas. On the other hand, recharge may increase due to the increased import or impoundment of surface water in the basins, which could give rise to more groundwater recharge from these surface water storages or indirectly when wastewater is discharged after use into unlined canals, wastewater treatment ponds, etc. Large water losses from inefficient urban water supply distribution systems could also enhance recharge (Birhanu et al. 2021). As urbanization increases, and reliance on groundwater grows, as exemplified by Addis Ababa, the net result may be a decrease in groundwater storage. In any case, urbanization would also imply a larger contamination load and pressure on groundwater resources, e.g., from poor solid waste and sanitation management. Understanding these processes and policy implications is vital to ensure sustainable groundwater use in urban contexts (Healy et al. 2022).

3. **Land cover change towards more irrigated agriculture**

The second-largest relative land cover change is conversion to larger irrigated agricultural areas (increase of 138% and 128% in UGRRB and UARB, respectively). The impact of this change on groundwater resources largely depends on the source of water for these expanded irrigated areas. If these areas are primarily served by surface water, groundwater levels and groundwater outflow to surface water bodies from significant irrigation return flows, as observed in the Awash Basin (Kebede et al. 2021), could take place. However, as groundwater is increasingly used as the sole or supplementary source of irrigation water, there is a risk of further depleting the resource. Groundwater quality may also be impaired significantly as a result of these land cover changes. More agrochemical leaching (from fertilizers and pesticides) from soils and more salinity due to lower river flows to dilute salts are some of the potential harmful consequences to groundwater resources. There is a need to use groundwater and surface water conjunctively (Birhanu et al. 2021) to increase irrigation and water-use efficiency (Birhanu et al. 2021), and to provide capacity and incentives for more land restoration and regenerative agriculture (Reij 2015).

In addition, climate change impacts may influence groundwater resources. Extreme rainfall events may increase infiltration potential, due to lower evapotranspiration losses and more focused recharge and preferential flow into the subsurface (Cuthbert et al. 2019). However, intensive rainfall may also accelerate surface runoff and increase soil erosion, hampering diffuse recharge, especially in degraded highlands. Climate change is possibly compounding the effects of land cover changes (e.g., land degradation) and intensified water demand, especially for irrigation, in extended drought periods (Daba and You 2022). Climate change is possibly also enhancing the risks of groundwater contamination due to flooding intercepting human waste and poorly-packaged, stored or soil-applied chemicals (Geris et al. 2022).

Conclusions

Land cover change in a traditional agropastoral landscape like that found in the Upper Great Ruaha River Basin (UGRRB) in Tanzania and the Upper Awash River Basin (UARB) in Ethiopia involves transitions from natural landscapes to intensively utilized landscapes, associated with population growth, economic development and the evolution of more complex production systems.

The pace of these transitions varies vastly between regions based on their historical, geographical, ecological, social and political characteristics, but with some common features, as observed in this study. Examples include the early transition to rainfed agriculture, shifting to increasing levels of irrigated agriculture, and agricultural, mostly rainfed, areas gradually giving way to human settlement/urban areas. Climate change may modify certain trajectories, as impacts on resources are manifested and human demands change.

Except in heavily built-up environments and intensive irrigation systems, the transitions are not always unidirectional. Investigating the multiple trajectories is necessary to comprehend the underlying patterns and overall land cover changes.

The analysis, covering the period 1995-2015, shows that UGRRB and UARB, broadly speaking, are at two successive stages of transition to more urbanized and more intensive farming systems, which is consistent with the findings from previous studies in low-income countries (Damtew et al. 2022; How Jin Aik et al. 2021). While UGRRB is still dominated by natural land cover (75% in 2015-2016), the natural land cover in UARB is almost vanishing (15% in 2015). The transition from natural ecosystems to agropastoral systems and further to urban systems supported by intensive agriculture is similar in both basins, but at successive stages, with UARB being at a more advanced stage. However, it must be noted that intensive irrigated agriculture already expanded in UGRRB early on, from the 1970s.

Another notable feature is that UARB has predominant land cover changes towards the perimeter (i.e., the highlands and headwaters of the basin), making it subject to land degradation and soil erosion. However, in UGRRB, development appears more concentrated towards the central plains, where there is still unutilized land and water resources, though the ecological functioning of the vital wetland and downstream conservation areas and hydropower infrastructure are already stressed. This trend appears partially tempered by a significant observed greening trend, presumably driven by a policy change to expand the Ruaha National Park in 2008.

Though not investigated in detail, the results indicate the need for analyzing land cover changes in these upper basins in a broader basin-scale context. There is a critical need to understand not only simple land cover changes, but also broader ecological, water consumption and water resources, and developmental and socioeconomic issues at the larger basin scale.

Observed land cover changes may affect and be affected by water use. As the reliance on groundwater for meeting human demands increases, while maintaining its role in providing ecosystem services remains critical, it is vital to understand the implications of land cover changes for this resource in these increasingly stressed basins and under climate change.

More broadly, the results of this study provide water resource managers and land use planners with valuable information to improve future land use and land cover policies and practices and develop basin management strategies for the UGRRB and UARB, with the goal of enhancing equitable and sustainable water and land resource use and building resilience.

References

Awulachew, S.B.; Yilma, A.D.; Loulseged, M.; Loiskandl, W.; Ayana, M.; Alamirew, T. 2007. *Water resources and irrigation development in Ethiopia*. Colombo, Sri Lanka: International Water Management Institute. 78p. (IWMI Working Paper 123). https://doi.org/10.3910/2009.305

Berhe, F.T.; Melesse, A.M.; Hailu, D.; Sileshi, Y. 2013. MODISM-based water allocation modeling of Awash River Basin, Ethiopia. *Catena* 109:118–128. https://doi.org/10.1016/j.catena.2013.04.007

Beyene, S.K.; Kemal, A.; Pingale, S.M. 2018. Impact of land use/land cover change on watershed hydrology: A case study of Upper Awash Basin, Ethiopia. *Ethiopian Journal of Water Science and Technology* 1(1):3–26.

Birhanu, B.; Kebede, S.; Charles, K.; Taye, M.; Atlaw, A.; Birhane, M. 2021. Impact of natural and anthropogenic stresses on surface and groundwater supply sources of the Upper Awash Sub-Basin, Central Ethiopia. *Frontiers In Earth Science* 9:656726. https://doi.org/10.3389/feart.2021.656726

Braune, E.; Xu, Y. 2010. The role of ground water in sub-Saharan Africa. *Groundwater* 48(2):229–238. https://doi.org/10.1111/j.1745-6584.2009.00557.x

Breiman, L. 2001. Random forests. *Machine Learning* 45(1):5–32. https://doi.org/10.1023/A:1010933404324

CIESIN (Center for International Earth Science Information Network, Columbia University). 2017. Gridded Population of the World, Version 4 (GPWv4): Population Count, Revision 10. Palisades, New York: National Aeronautics and Space Administration (NASA) Socioeconomic Data and Applications Center (SEDAC). https://doi.org/10.7927/H4PG1PPM

Chance, E.W.; Cobourn, K.M.; Thomas, V.A.; Dawson, B.C.; Flores, A.N. 2017. Identifying irrigated areas in the Snake River Plain, Idaho: Evaluating performance across composting algorithms, spectral indices, and sensors. *Remote Sensing* 9(6):546. https://doi.org/10.3390/rs9060546

Cuthbert, M.O.; Taylor, R.G.; Favreau, G.; Todd, M.C.; Shamsudduha, M.; Villholth, K.G.; MacDonald, A.M.; Scanlon, B.R.; Valerie Kotchoni, D.O.; Vouillamoz, J.-M.; Lawson, F.M.A.; Adjomayi, P.A.; Kashaigili, J.; Seddon, D.; Sorensen, J.P.R.; Ebrahim, G.Y.; Owor, M.; Nyenje, P.M.; Nazoumou, Y.; Goni, I.; Ousmane, B.I.; Sibanda, T.; Ascott, M.J.; Macdonald, D.M.J.; Agyekum, W.; Koussoubé, Y.; Wanke, H.; Kim, H.; Wada, Y.; Lo, M.-H.; Oki, T.; Kukuric, N. 2019. Observed controls on resilience of groundwater to climate variability in sub-Saharan Africa. *Nature* 572:230–234. https://doi.org/10.1038/s41586-019-1441-7

Daba, M.H.; You, S. 2022. Quantitatively assessing the future land-use/land-cover changes and their driving factors in the upper stream of the Awash River based on the CA–Markov model and their implications for water resources management. *Sustainability* 14(3):1538. https://doi.org/10.3390/su14031538

Damtew, A.; Teferi, E.; Ongoma, V. 2022. Farmers' perceptions and spatial statistical modeling of most systematic LULC transitions: Drivers and livelihood implications in Awash Basin, Ethiopia. *Remote Sensing Applications: Society and Environment* 25:100661. https://doi.org/10.1016/j.rsase.2021.100661

Edossa, D.C.; Babel, M.S.; Gupta, A.D. 2010. Drought analysis in the Awash River Basin, Ethiopia. *Water Resources Management* 24:1441–1460. https://doi.org/10.1007/s11269-009-9508-0

Egorov, A.V.; Hansen, M.C.; Roy, D.P.; Kommareddy, A.; Potapov, P.V.; 2015. Image interpretation-guided supervised classification using nested segmentation. *Remote Sensing of Environment* 165: 135–147. https://doi.org/10.1016/j.rse.2015.04.022

Eklundh, L.; Olsson, L. 2003. Vegetation index trends for the African Sahel 1982 – 1999. *Geophysical Research Letters* 30(8):1430. https://doi.org/10.1029/2002GL016772

Favreau, G.; Cappelaere, B.; Massuel, S.; Leblanc, M.; Boucher, M.; Boulain, N.; Leduc, C. 2009. Land clearing, climate variability, and water resources increase in semiarid southwest Niger: A review. *Water Resources Research* 45(7): W00A16. https://doi.org/10.1029/2007WR006785

Fensholt, R.; Langanke, T.; Rasmussen, K.; Reenberg, A.; Prince, S.D.; Tucker, C.; Scholes, R.J.; Le, Q.B.; Bondeau, A.; Eastman, R.; Epstein, H.; Gaughan, A.E.; Hellden, U.; Mbow, C.; Olsson, L.; Paruelo, J.; Schweitzer, C.; Seaquist, J.; Wessels, K. 2012. Greenness in semi-arid areas across the globe 1981–2007 — an Earth Observing Satellite based analysis of trends and drivers. *Remote Sensing of Environment* 121:144–158. https://doi.org/10.1016/j.rse.2012.01.017

Fierens, F.; Rosin, P.L. 1994. Filtering remote sensing data in the spatial and feature domains. In: Desachy, J. (ed.) *Proceedings of SPIE Vol. 2315. Image and signal processing for remote sensing*. pp.472–482. https://doi.org/10.1117/12.196747

FAO (Food and Agriculture Organization of the United Nations). 1965. *Report on survey of the Awash River Basin. Volume IV: Water storage and power development*. Imperial Ethiopian Government United Nations Special Fund Project. Rome: Food and Agriculture Organization of the United Nations (FAO).

FAO. 2011. *The state of the world's land and water resources for food and agriculture (SOLAW) – Managing systems at risk*. Rome: Food and Agriculture Organization of the United Nations (FAO) and London: Earthscan.

FAO. 2015. Global Administrative Unit Layers (GAUL). Rome: Food and Agriculture Organization of the United Nations (FAO). Available at https://data.apps.fao.org/map/catalog/srv/eng/catalog.search?id=12691#/metadata/9c35ba10-5649-41c8-bdfc-eb78e9e65654 (accessed on March 23, 2023).

Gashaw, T.; Tulu, T.; Argaw, M.; Worqlul, A.W. 2017. Evaluation and prediction of land use/land cover changes in the Andassa watershed, Blue Nile Basin, Ethiopia. *Environmental Systems Research* 6:17. https://doi.org/10.1186/s40068-017-0094-5

Gedefaw, M.; Wang, H.; Yan, D.; Qin, T.; Wang, K.; Girma, A.; Batsuren, D.; Abiyu, A. 2019. Water resources allocation systems under irrigation expansion and climate change scenario in Awash River basin of Ethiopia. *Water* 11(10):1966. https://doi.org/10.3390/w11101966

Geris, J.; Comte, J.-C.; Franchi, F.; Petros, A.K.; Tirivarombo, S.; Selepeng, A.T.; Villholth, K.G. 2022. Surface water-groundwater interactions and local land use control water quality impacts of extreme rainfall and flooding in a vulnerable semi-arid region of Sub-Saharan Africa. *Journal of Hydrology* 609:127834. https://doi.org/10.1016/j.jhydrol.2022.127834

Hassen, E.E.; Assen, M. 2018. Land use/cover dynamics and its drivers in Gelda catchment, Lake Tana watershed, Ethiopia. *Environmental Systems Research* 6:4. https://doi.org/10.1186/s40068-017-0081-x

He, C.; Shi, P.; Xie, D.; Zhao, Y. 2010. Improving the normalized difference built-up index to map urban built-up areas using a semiautomatic segmentation approach. *Remote Sensing Letters* 1(4):213–221. https://doi.org/10.1080/01431161.2010.481681

Healy, A.; Tijani, M.; Grönwall, J.; Eichholz, M.; Villholth, K.G.; Mwango, F.; Danert, K.; Upton, K.; Lapworth, D.; Lalika, M.C.S.; Gicheruh, C. 2022. *Urban groundwater in Africa: A dialogue for resilient towns and cities*. AMCOW Pan-African Groundwater Programme (APAGroP). Abuja, Nigeria: African Ministers' Council on Water (AMCOW).

Hickler, T.; Eklundh, L.; Seaquist, J.W.; Smith, B.; Ardö, J.; Olsson, L.; Sykes, M.T.; Sjöström, M. 2005. Precipitation controls Sahel greening trend. *Geophysical Research Letters* 32(21):L21415. https://doi.org/10.1029/2005GL024370

How Jin Aik, D.; Ismail, M.H; Muharam, F.M.; Alias, M.A. 2021. Evaluating the impacts of land use/land cover changes across topography against land surface temperature in Cameron Highlands. *PLoS ONE* 16(5): e0252111. https://doi.org/10.1371/journal.pone.0252111

Huber S.; Fensholt, R.; Rasmussen, K. 2011. Water availability as the driver of vegetation dynamics in the African Sahel from 1982 to 2007. *Global and Planetary Change* 76(3–4):186–195. https://doi.org/10.1016/j.gloplacha.2011.01.006

Huete, A.R. 1988. A soil-adjusted vegetation index (SAVI). *Remote Sensing of Environment* 25(3):295–309. https://doi.org/10.1016/0034-4257(88)90106-X

Hurni, H.; Tato, K.; Zeleke, G. 2005. The implications of changes in population, land use, and land management for surface runoff in the Upper Nile Basin area of Ethiopia. *Mountain Research and Development* 25(2):147–154. https://doi.org/10.1659/0276-4741(2005)025[0147:TIOCIP]2.0.CO;2

Hyandye, C.B. 2019. *Impacts of future climate and landuse changes on surface-groundwater balance in Usangu catchment*. PhD Thesis. Arusha, Tanzania: The Nelson Mandela African Institution of Science and Technology. 192p.

IPBES (Intergovernmental Science-Policy Platform on Biodiversity and Ecosystem Services). 2019. *Summary for policymakers of the global assessment report on biodiversity and ecosystem services of the Intergovernmental Science-Policy Platform on Biodiversity and Ecosystem Services*. Díaz, S.; Settele, J.; Brondízio, E.S.; Ngo, H.T.; Guèze, M.; Agard, J.; Arneth, A.; Balvanera, P.; Brauman, K.A.; Butchart, S.H.M.; Chan, K.M.A.; Garibaldi, L.A.; Ichii, K.; Liu, J.; Subramanian, S.M.; Midgley, G.F.; Miloslavich, P.; Molnár, Z.; Obura, D.; Pfaff, A.; Polasky, S.; Purvis, A.; Razzaque, J.; Reyers, B.; Roy Chowdhury, R.; Shin, Y.J.; Visseren-Hamakers, I.J.; Willis, K.J.; Zayas, C.N. (eds.). Bonn, Germany: IPBES secretariat. 56p.

Jensen, J.R. 1996. *Introductory digital image processing: A remote sensing perspective*. *2nd edition*. New Jersey, USA: Prentice-Hall.

Kashaigili, J.J. 2008. Impacts of land-use and land-cover changes on flow regimes of the Usangu wetland and the Great Ruaha River, Tanzania. *Physics and Chemistry of the Earth, Parts A/B/C* 33(8-13):640–647. https://doi.org/10.1016/j.pce.2008.06.014

Kashaigili, J.J.; McCartney, M.P.; Mahoo, H.F.; Lankford, B.A.; Mbilinyi, B.P.; Yawson, D.K.; Tumbo, S.D. 2006a. *Use of a hydrological model for environmental management of the Usangu wetlands, Tanzania*. Colombo, Sri Lanka: International Water Management Institute (IWMI). 48p. (IWMI Research Report 104). https://doi.org/10.3910/2009.104

Kashaigili, J.J.; Mbilinyi, B.P.; McCartney, M.; Mwanuzi, F.L. 2006b. Dynamics of Usangu plains wetlands: Use of remote sensing and GIS as management decision tools. *Physics and Chemistry of the Earth, Parts A/B/C* 31(15–16): 967–975. https://doi.org/10.1016/j.pce.2006.08.007

Kashaigili, J.J.; Rajabu, K.; Masolwa, P. 2009. Freshwater management and climate change adaptation: Experiences from the Great Ruaha River catchment in Tanzania. *Climate and Development* 1(3):220–228. https://doi.org/10.3763/cdev.2009.0025

Kebede, S.; Charles, K.; Godfrey, S.; MacDonald, A.; Taylor, R.G.; 2021. Regional-scale interactions between groundwater and surface water under changing aridity: Evidence from the River Awash Basin, Ethiopia. *Hydrological Sciences Journal* 66(3):450–463, https://doi.org/10.1080/02626667.2021.1874613

Kihwele, E.; Mnaya, B.; Meng'ataki, G.; Birkett, C.; Wolanski, E. 2012. The role of vegetation in the water budget of the Usangu wetlands, Tanzania. *Wetlands Ecology and Management* 20(5):389–398. http://dx.doi.org/10.1007/s11273-012-9260-8

Kihwele, E.; Muse, E.; Magomba, E.; Mnaya, B.; Nassoro, A.; Banga, P.; Murashani, E.; Irmamasita, D.; Kiwango, H.; Birkett, C.; Wolanski, E. 2018. Restoring the perennial Great Ruaha River using ecohydrology, engineering and governance methods in Tanzania. *Ecohydrology and Hydrobiology* 18(2):120–129. https://doi.org/10.1016/j.ecohyd.2017.10.008

Krishnaswamy, J.; Kiran, M.C.; Ganeshaiah, K.N. 2004. Tree model based eco-climatic vegetation classification and fuzzy mapping in diverse tropical deciduous ecosystems using multi-season NDVI. *International Journal of Remote Sensing* 25(6):1185–1205. https://doi.org/10.1080/0143116031000149989

Lambin, E.F.; Meyfroidt, P. 2011. Global land use change, economic globalization, and the looming land scarcity. *Proceedings of the National Academy of Sciences* 108(9):3465–3472. https://doi.org/10.1073/pnas.1100480108

Lu, D.; Mausel, P.; Brondízio, E.; Moran, E. 2004. Change detection techniques. *International Journal of Remote Sensing* 25(12):2365–2401. https://doi.org/10.1080/0143116031000139863

Lyon, J.G.; Yuan, D.; Lunetta, R.S.; Elvidge, C.D. 1998. A change detection experiment using vegetation indices. *Photogrammetric Engineering and Remote Sensing* 64(2):143–150.

Matima, J.M.; Mugatha, S.M.; Reid, R.S.; Gachimbi, L.N.; Majule, A.; Lyaruu, H.; Pomery, D.; Mathai, S.; Mugisha, S. 2009. The linkages between land use change, land degradation and biodiversity across East Africa. *African Journal of Environmental Science and Technology* 3(10):310–325.

Mekuria, W.; Veldkamp, E.; Haile, M.; Gebrehiwot, K.; Muys, B.; Nyssen, J. 2009. Effectiveness of exclosures to control soil erosion and local community perception on soil erosion in Tigray, Ethiopia. *African Journal of Agricultural Research* 4(4):365–377.

Millennium Ecosystem Assessment. 2005. *Ecosystems and human well-being: Synthesis*. Washington, DC, USA: Island Press.

Mtibaa, S.; Irie, M. 2016. Land cover mapping in cropland dominated area using information on vegetation phenology and multi-seasonal Landsat 8 images. *Euro-Mediterranean Journal for Environmental Integration* 1(6). https://doi.org/10.1007/s41207-016-0006-5

Mwakalila, S. 2011. Vulnerability of people's livelihoods to water resources availability in semi-arid areas of Tanzania. *Journal of Water Resource and Protection* 3(9):678–685. https://doi.org/10.4236/jwarp.2011.39078

NASA JPL (National Aeronautics and Space Administration Jet Propulsion Laboratory). 2013. *NASA Shuttle Radar Topography Mission Global 1 arc second* [Data set]. Distributed by NASA EOSDIS Land Processes DAAC. https://doi.org/10.5067/MEaSUREs/SRTM/SRTMGL1.003 (accessed on August 10, 2022).

NEMC (National Environment Management Council). 2006. *Integrated ecosystems assessment in Tanzania: Experiences in ecosystems management*. Dar es Salaam, Tanzania: National Environment Management Council (NEMC).

Oqubay, A. 2018. *Industrial policy and late industrialization in Ethiopia*. Working Paper Series N° 303. Abidjan, Côte d'Ivoire: African Development Bank.

Qi, J.; Chehbouni, A.; Huete, A.R.; Kerr, Y.H.; Sorooshian, S. 1994. A modified soil adjusted vegetation index. *Remote Sensing of Environment* 48(2):119–126. https://doi.org/10.1016/0034-4257(94)90134-1

Reed, B.C.; Brown, J.F.; VanderZee, D.; Loveland, T.R.; Merchant, J.W.; Ohlen, D.O. 1994. Measuring phenological variability from satellite imagery. *Journal of Vegetation Science* 5(5):703–714. https://doi.org/10.2307/3235884

Reij, C. 2015. How Ethiopia went from famine crisis to green revolution. *Insights*, July 28, 2015. Washington, DC, USA: World Resources Institute (WRI). Available at https://www.wri.org/insights/how-ethiopia-went-famine-crisis-green-revolution (accessed on February 20, 2022).

Senf, C.; Leitão, P.J.; Pflugmacher, D.; van der Linden, S.; Hostert, P. 2015. Mapping land cover in complex Mediterranean landscapes using Landsat: Improved classification accuracies from integrating multi-seasonal and synthetic imagery. *Remote Sensing of Environment* 156:527–536. https://doi.org/10.1016/j.rse.2014.10.018

Seto, K.C.; Fragkias, M.; Güneralp, B.; Reilly, M.K. 2011. A meta-analysis of global urban land expansion. *PLoS ONE* 6(8):e23777. https://doi.org/10.1371/journal.pone.0023777

Settle, J.J.; Briggs, S.A. 1987. Fast maximum likelihood classification of remotely-sensed imagery. *International Journal of Remote Sensing* 8(5):723-734. https://doi.org/10.1080/01431168708948683

Sharma, A.K.; Hubert-Moy, L.; Buvaneshwari, S.; Sekhar, M.; Ruiz, L.; Bandyopadhyay, S.; Corgne, S. 2018. Irrigation history estimation using multitemporal Landsat satellite images: Application to an Intensive groundwater irrigated agricultural watershed in India. *Remote Sensing* 10(6):893. https://doi.org/10.3390/rs10060893

Sosovele, H.; Ngwale, J.J. 2002. *Socio-economic root causes of the loss of biodiversity in the Ruaha catchment area*. Report submitted to WWF-Tanzania. Available at http://assets.panda.org/downloads/rcareportruaha.pdf (accessed on March 9, 2020).

Stears, K.; McCauley, D.J.; Finlay, J.C.; Mpemba, J.; Warrington, I.T.; Mutayoba, B.M.; Power, M.E.; Dawson, T.E.; Brashares, J.S. 2018. Effects of the hippopotamus on the chemistry and ecology of a changing watershed. *Proceedings of the National Academy of Sciences* 115(22): E5028-E5037. https://doi.org/10.1073/pnas.1800407115

Story, M.; Congalton, R.G. 1986. Accuracy assessment: A user's perspective. *Photogrammetric Engineering and Remote Sensing* 52(3):397–399.

SMUWC (Sustainable Management of Usangu Wetlands and its Catchment). 2001a. *Final report – Annex 1: Baseline 2001*. Dar es Salaam, Tanzania: Directorate of Water Resources. Available at https://web.archive.org/web/20031206152634/http://www.usangu.org/pdf/baseline2001.pdf (accessed on March 5, 2023)

SMUWC. 2001b. *Water resources. Supporting report 7, Volume 3*. Dar es Salaam, Tanzania: Directorate of Water Resources. 209p. Available at https://resources.bgs.ac.uk/sadcreports/tanzania2001smuwcusangubasinirrigation.pdf (accessed on March 5, 2023)

Swain, P.H.; Davis, S.M. (Eds.) 1978. *Remote sensing: The quantitative approach*. New York: McGraw Hill Book Company. 396p.

Taylor, A.; Rubena, J.; Masanja, M.; Devisscher, T.; Jeans, H. 2011. *Final report: Tanzania study –ecosystems, development, and climate adaptation: Improving the knowledge base for policies, planning and management*. SEI final project report to WWF. Oxford, UK: Stockholm Environmental Institute (SEI). 30p.

Taylor, R.G.; Scanlon, B.; Döll, P.; Rodell, M.; van Beek, R.; Wada, Y.; Longuevergne, L.; Leblanc, M.; Famiglietti, J.S.; Edmunds, M.; Konikow, L.; Green, T.R.; Chen, J.; Taniguchi, M.; Bierkens, M.F.P.; MacDonald, A.; Fan, Y.; Maxwell, R.M.; Yechieli, Y.; Gurdak, J.J.; Allen, D.M.; Shamsudduha, M.; Hiscock, K.; Yeh, P.J.-F.; Holman, I.; Treidel, H. 2013. Ground water and climate change. *Nature Climate Change* 3: 322–329. https://doi.org/10.1038/nclimate1744

UN DESA (United Nations Department of Economic and Social Affairs). 2015. *World population prospects: The 2015 revision, key findings and advance tables*. Working Paper No. ESA/P/WP.241. New York: United Nations, Department of Economic and Social Affairs, Population Division.

USGS (United States Geological Survey). n.d.(a). Normalized Difference Moisture Index. Available at https://www.usgs.gov/landsat-missions/normalized-difference-moisture-index (accessed on March 5, 2023)

USGS. n.d.(b). *What are the band designations for the Landsat satellites?* Available at https://www.usgs.gov/faqs/what-are-band-designations-landsat-satellites (accessed on March 5, 2023).

USGS. 2015. *Landsat surface reflectance data (version 1.1, March 2019)*. U.S. Geological Survey Fact Sheet 2015-3034. 1p. http://dx.doi.org/10.3133/fs20153034

USGS. 2016a. *Landsat—Earth observation satellites (ver. 1.1, August 2016)*. U.S. Geological Survey Fact Sheet 2015-3081. 4p. Archived from the Wayback Machine on https://web.archive.org/web/20170218030422/https://pubs.usgs.gov/fs/2015/3081/fs20153081.pdf (accessed on May 23, 2023).

USGS. 2016b. EarthExplorer (internet data archive). Available at https://earthexplorer.usgs.gov/ (accessed on August 10, 2022).

USGS. 2019. *Landsat 8 (L8) data users handbook, version 5.0*. Reston, Virginia, USA: Department of the Interior, United States Geological Survey. Available at https://www.usgs.gov/media/files/landsat-8-data-users-handbook (accessed on March 5, 2023).

USGS. 2020a. *Landsat 4-7 Collection 1 (C1) surface reflectance (LEDAPS): Product guide*, version 3. Reston, Virginia, USA: Department of the Interior, United States Geological Survey. Available at https://www.usgs.gov/media/files/landsat-4-7-collection-1-surface-reflectance-code-ledaps-product-guide (accessed on March 5, 2023)

USGS. 2020b. *Landsat 8 Collection 1 (C1) Land Surface Reflectance Code (LaSRC): Product guide*, version 3. Reston, Virginia, USA: Department of the Interior, United States Geological Survey. Available at https://www.usgs.gov/media/files/landsat-8-collection-1-land-surface-reflectance-code-product-guide (accessed on March 5, 2023).

Vesa, L.; Malimbwi, R.E.; Tomppo, E.; Zahabu, E.; Maliondo, S.; Chamuya, N.; Nssoko, E.; Otieno, J.; Miceli, G.; Kaaya, A.K.; Dalsgaard, S. 2011. *National Forestry Resources Monitoring and Assessment of Tanzania (NAFORMA): Field manual – Biophysical survey*. Dar es Salaam, Tanzania: Forestry and Beekeeping Division, Ministry of Natural Resources and Tourism, The United Republic of Tanzania.

Villholth, K.G.; Ganeshamoorthy, J.; Rundblad, C.M.; Knudsen, T.S. 2013. Smallholder groundwater irrigation in sub-Saharan Africa: An interdisciplinary framework applied to the Usangu plains, Tanzania. *Hydrogeology Journal* 21(7):1481–1495. https://doi.org/10.1007/s10040-013-1016-x

Walsh, M. 2012. The not-so-Great Ruaha and hidden histories of an environmental panic in Tanzania. *Journal of Eastern African Studies* 6(2):303–335. https://doi.org/10.1080/17531055.2012.669575

Wardlow, B.D.; Egbert, S.L. 2008. Large-area crop mapping using time-series MODIS 250 m NDVI data: An assessment for the U.S. Central Great Plains. *Remote Sensing of Environment* 112(3):1096–1116. https://doi.org/10.1016/j.rse.2007.07.019

Wilson, E.H.; Sader, S.A. 2002. Detection of forest harvest type using multiple dates of Landsat TM imagery. *Remote Sensing of Environment* 80(3):385–396. https://doi.org/10.1016/S0034-4257(01)00318-2

Worqlul, A.W.; Jeong, J.; Dile, Y.T.; Osorio, J.; Schmitter, P.; Gerik, T.; Srinivasan, R.; Clark, N. 2017. Assessing potential land suitable for surface irrigation using groundwater in Ethiopia. *Applied Geography* 85:1–13. http://dx.doi.org/10.1016/j.apgeog.2017.05.010

Zeleke, G.; Hurni, H. 2001. Implications of land use and land cover dynamics for mountain resource degradation in the northwestern Ethiopian highlands. *Mountain Research and Development* 21(2):184–191. https://doi.org/10.1659/0276-4741(2001)021[0184:IOLUAL]2.0.CO;2

Zha, Y.; Gao, J.; Ni, S. 2003. Use of normalized difference built-up index in automatically mapping urban areas from TM imagery. *International Journal of Remote Sensing* 24(3):583–594.

Appendix. Characteristics of Landsat Images and Data Access.

The Landsat program is a land remote sensing program jointly operated by the National Aeronautics and Space Administration (NASA) and the United States Geological Survey (USGS) from 1972 onwards. Eight satellites have been launched at various points of time as part of the continuous program, in which Landsat 7 and Landsat 8 are currently operational (as at 2017). This study used images from Landsat 5, 7 and 8 satellites.

The Landsat images and surface reflectance data products derived from these images are available to download from the online data archive EarthExplorer.[9] EarthExplorer, maintained by USGS, provides a convenient interface for users to search, order and download remote sensing data from several sensors, including various Landsat sensors.

Landsat 8

Landsat 8 is the latest satellite in the series, which was launched in February 2013. Landsat 8 has a 16-day revisit cycle and carries two push-broom instruments: the Operational Land Imager (OLI) and Thermal Infrared Sensor (TIRS). The OLI sensor collects image data in nine spectral bands and TIRS collects data in two thermal bands over a 190 km swath. Details of the Landsat 8 mission can be found in the Landsat 8 Data Users Handbook (USGS 2019). The characteristics of OLI and TIRS spectral bands are provided in Table A1.

Table A1. Band designations of the Landsat 8 satellite.

Band number	Band name	Wavelength (10^{-6} m)	Spatial resolution (m)
Band 1	Coastal/Aerosol (CA)	0.435 - 0.451	30
Band 2	Blue	0.452 - 0.512	30
Band 3	Green	0.533 - 0.590	30
Band 4	Red	0.636 - 0.673	30
Band 5	Near Infrared (NIR)	0.851 - 0.879	30
Band 6	Shortwave Infrared (SWIR) 1	1.566 - 1.651	30
Band 7	Shortwave Infrared (SWIR) 2	2.107 - 2.294	30
Band 8	Panchromatic	0.503 - 0.676	15
Band 9	Cirrus	1.363 - 1.384	30
Band 10	Thermal Infrared Sensor (TIRS) 1	10.60 - 11.19	100* (30)
Band 11	Thermal Infrared Sensor (TIRS) 2	11.50 - 12.51	100* (30)

Source: USGS n.d.(b)

Note: * TIRS bands are acquired at 100 m resolution, but the data products are resampled to 30 m pixels.

Landsat 7

The Landsat Enhanced Thematic Mapper Plus (ETM+) sensor is carried on the Landsat 7 satellite, which was launched in April 1999. The sensor suffered a scan line corrector (SLC) failure in 2003, which resulted in a loss of data in the acquired images from that point onwards. Landsat 7 has a 16-day revisit cycle and the swath width is 183 km x 170 km. The Landsat ETM+ spectral bands are given in Table A2.

[9] https://earthexplorer.usgs.gov/

Table A2. Band designations of the Landsat 7 satellite.

Band number	Band name	Wavelength (10^{-6} m)	Spatial resolution (m)
Band 1	Blue	0.45 - 0.52	30
Band 2	Green	0.52 - 0.60	30
Band 3	Red	0.63 - 0.69	30
Band 4	Near Infrared (NIR)	0.77 - 0.90	30
Band 5	Shortwave Infrared (SWIR) 1	1.55 - 1.75	30
Band 6	Thermal	10.40 - 12.50	60* (30)
Band 7	Shortwave Infrared (SWIR) 2	2.09 - 2.35	30
Band 8	Panchromatic	0.52 - 0.90	15

Source: USGS n.d.(b)

Note: * ETM+ Band 6 was acquired at 60 m resolution, but the data products are resampled to 30 m pixels.

Landsat 5

The Landsat Thematic Mapper (TM) carried on the Landsat 5 satellite was operational from March 1984 to January 2013, and provided images acquired in seven spectral bands. Landsat 5 had a 16-day revisit cycle and the swath width was 185 km. The Landsat TM spectral bands are given in Table A3.

Table A3. Band designations of the Landsat 5 satellite.

Band number	Band name	Wavelength (10^{-6} m)	Spatial resolution (m)
Band 1	Blue	0.45 - 0.52	30
Band 2	Green	0.52 - 0.60	30
Band 3	Red	0.63 - 0.69	30
Band 4	Near Infrared (NIR)	0.76 - 0.90	30
Band 5	Shortwave Infrared (SWIR) 1	1.55 - 1.75	30
Band 6	Thermal	10.40 - 12.50	120* (30)
Band 7	Shortwave Infrared (SWIR) 2	2.08 - 2.35	30

Source: USGS n.d.(b)

Note: * TM Band 6 was acquired at 120 m resolution, but the data products are resampled to 30 m pixels.

Landsat Surface Reflectance Products

Landsat Surface Reflectance data products provided by USGS were used to develop various spectral indices for the classification. Surface reflectance data are produced after the removal of atmospheric artefacts on satellite data. Removing atmospheric effects make remote sensing data acquired from various locations and various time periods comparable. The Surface Reflectance data for Landsat 5 and 7 were developed by using Landsat Ecosystem Disturbance Adaptive Processing System (LEDAPS) (USGS 2020a), whereas Landsat 8 OLI surface reflectance data are generated through the Land Surface Reflectance Code (LaSRC) (USGS 2020b) algorithm.

IWMI Research Report Series

184 Land Cover Changes in the Upper Great Ruaha (Tanzania) and the Upper Awash (Ethiopia) River Basins and their Potential Implications for Groundwater Resources
https://doi.org/10.5337/2023.212

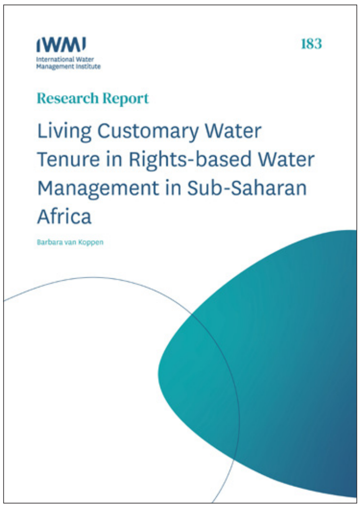

183 Living Customary Water Tenure in Rights-based Water Management in Sub-Saharan Africa
https://doi.org/10.5337/2022.214

182 Legal Recognition of Customary Water Tenure in Sub-Saharan Africa: Unpacking the Land-Water Nexus
https://doi.org/10.5337/2022.215

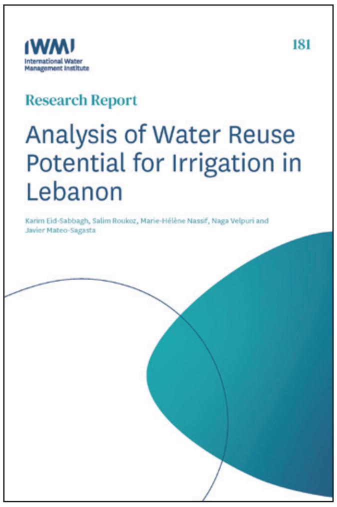

181 Analysis of Water Reuse Potential for Irrigation in Lebanon
https://doi.org/10.5337/2022.211

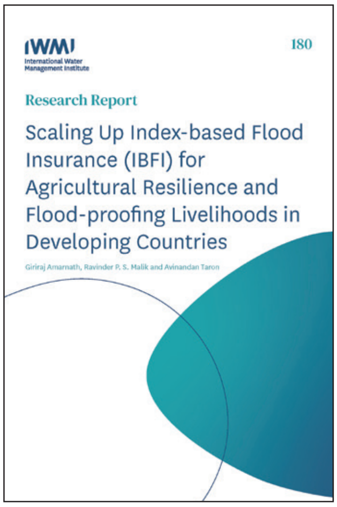

180 Scaling Up Index-based Flood Insurance for Agricultural Resilience and Flood-proofing Livelihoods in Developing Countries
https://doi.org/10.5337/2021.213

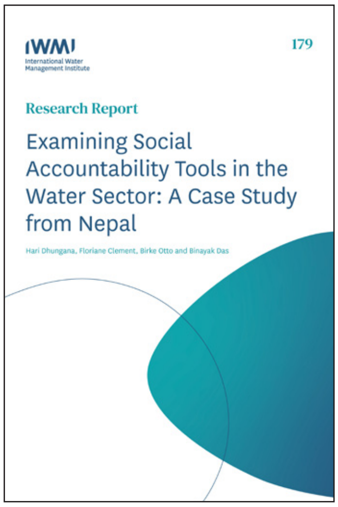

179 Examining Social Accountability Tools in the Water Sector: A Case Study from Nepal
https://doi.org/10.5337/2021.211

For access to all IWMI publications, visit www.iwmi.org/publications/

Headquarters
127 Sunil Mawatha
Pelawatta
Battaramulla
Sri Lanka

Mailing address
P. O. Box 2075
Colombo
Sri Lanka

Telephone
+94 11 2880000

Fax
+94 11 2786854

Email
iwmi@cgiar.org

Website
www.iwmi.org

International Water Management Institute

IWMI is a CGIAR Research Center

ISSN 1026-0862
ISBN 978-92-9090-952-1